Environmental Pollution 239 (2018) 617–630

Contents lists available at ScienceDirect

Environmental Pollution

journal homepage: www.elsevier.com/locate/envpol

Mixed method approach to assess atmospheric nitrogen deposition in arid and semi-arid ecosystems☆

Elizabeth M. Cook [a, *, 1], Ryan Sponseller [b], Nancy B. Grimm [a, c], Sharon J. Hall [a, c]

[a] School of Life Sciences, Arizona State University, Tempe, AZ, 85287, USA
[b] Department of Ecology and Environmental Science, Umeå University, Umeå, Sweden
[c] Julie Ann Wrigley Global Institute of Sustainability, Arizona State University, Tempe, AZ, 85287, USA

ARTICLE INFO

Article history:
Received 21 September 2017
Received in revised form
12 March 2018
Accepted 3 April 2018

Keywords:
Inorganic nitrogen deposition
Aridland ecosystems
Dry deposition
Urban-rural gradient

ABSTRACT

Arid and semi-arid ecosystems (aridlands) cover a third of Earth's terrestrial surface and contain organisms that are sensitive to low level atmospheric pollutants. Atmospheric nitrogen (N) inputs to aridlands are likely to cause changes in plant community composition, fire frequency, and carbon cycling and storage. However, few studies have documented long-term rates of atmospheric N inputs in aridlands because dry deposition is technically difficult to quantify, and extensive sampling is needed to capture fluxes with spatially and temporally heterogeneous rainfall patterns. Here, we quantified long-term spatial and temporal patterns of inorganic N deposition in protected aridland ecosystems across an extensive urban-rural gradient using multiple sampling methods. We compared long-term rates of N deposition from ion-exchange resin (IER) collectors (bulk and throughfall, 2006–2015), wet-dry bucket collectors (2006–2015), and dry deposition from the inferential method using passive samplers (2010–2012). From mixed approaches with IER collectors and inferential methods, we determined that 7.2 ± 0.4 kgNha^{-1}y^{-1} is deposited to protected Sonoran Desert within metropolitan Phoenix, Arizona and 6.1 ± 0.3 kgNha^{-1}y^{-1} in nearby desert ecosystems. Regional scale models overestimated deposition rates for our sampling period by 60% and misidentified hot spots of deposition across the airshed. By contrast, the easy-deployment IER throughfall collectors showed minimal spatial variation across the urban-rural gradient and underestimated deposition fluxes by 54%, largely because of underestimated dry deposition in throughfall. However, seasonal sampling of the IER collectors over 10 years allowed us to capture significant seasonal variation in N deposition and the importance of precipitation timing. These results, derived from the longest, spatially and temporally explicit dataset in drylands, highlight the need for long-term, mixed methods to estimate atmospheric nutrient enrichment to aridlands in a rapidly changing world.

1. Introduction

Increased human activities have led to elevated concentrations of atmospheric reactive nitrogen (N) worldwide (Vitousek et al., 1997; Galloway et al., 2004; Dentener et al., 2006). N gas emissions from urban and agricultural sources are transported downwind and deposited upon surfaces through rainfall (wet deposition), cloud vapor, and adsorption of gases and particles (dry deposition). Increasing rates of N deposition during decades of agricultural and industrial growth, and the significant ecological consequences of increased rates, have been well characterized in ecosystems with high rainfall (Lovett, 1994; Aber et al., 1998; Galloway et al., 2004; Holland et al., 2005; Dentener et al., 2006; Phoenix et al., 2006; Weathers et al., 2006; Pardo et al., 2011). However, N deposition is also expected to increase in dryland ecosystems where a disproportionate amount of future urban growth is anticipated (United Nations, 2014). While arid and semi-arid ecosystems cover over a third of the globe's land area, far more effort has been put into quantifying patterns of N deposition to mesic compared to aridland ecosystems.

Although water constrains primary production in aridlands, N availability significantly affects ecosystem functioning during wet

☆ This paper has been recommended for acceptance by Dr. Hageman Kimberly Jill.
* Corresponding author.
E-mail address: Elizabeth.M.Cook@newschool.edu (E.M. Cook).
[1] Urban Systems Lab, Environmental Studies Department, The New School, New York, NY, 10003, USA (present address).

https://doi.org/10.1016/j.envpol.2018.04.013
0269-7491/

periods and within landscape patches with prolonged access to soil water (Hall et al., 2011; Ladwig et al., 2012; Collins et al., 2014). However, precipitation variability in drylands decouples plant and soil processes, making it unlikely that arid ecosystem functioning will respond to N deposition according to the forest N saturation model in temperate ecosystems (*sensu* Aber et al., 2002; Hall et al., 2011). The few studies examining the effects of elevated N inputs to arid ecosystems have reported increases in annual herbaceous (but not perennial) plant growth, losses of native vegetation, and greater fire frequency (Brooks, 2003; Fenn et al., 2003a; Báez et al., 2007; Rao et al., 2010; Hall et al., 2011). Such responses, particularly during wet periods, may have cascading effects on ecosystem services, including carbon storage (Ochoa-Hueso et al., 2013; Poulter et al., 2014). Many aridland ecosystems are predicted to receive atmospheric N inputs at or above the desert critical load, the threshold at which many ecological changes occur (Fenn et al., 2010; Pardo et al., 2011). Deposition rates as low as 3–9 $kgNha^{-1}y^{-1}$ can alter the seasonal growth and composition of herbaceous plant communities (Fenn et al., 2003a, 2010; Pardo et al., 2011; Simkin et al., 2016). By comparison, in central and southern California, United States (US)—one of the few places where aridland N deposition has been well studied—dry deposition alone is estimated to be as high as 14–35 $kgNha^{-1}y^{-1}$ (Alonso et al., 2005; Rao et al., 2009; Cisneros et al., 2010).

Long-term atmospheric deposition in aridlands is challenging to estimate in part due to the pulsed nature of precipitation, where episodic and often intense, rainfall events punctuate long dry periods (Noy-Meir, 1973; Collins et al., 2014). Despite this, long-term monitoring is important for evaluating ecosystem changes, conservation strategies, and policies controlling N emissions (Holland et al., 2005; Lovett, 2013). For example, since the 1990 US Clean Air Act amendments, the composition of N deposition in the US has changed from primarily oxidized N (e.g., nitrogen oxides (NO_x)) to reduced N forms (e.g., ammonia (NH_3); Du et al., 2014; Li et al., 2016; Lloret and Valiela, 2016), reflecting a broad shift from industrial to agriculture sources. While changing patterns of N deposition have been examined at the national scale, much less is known about regional long-term deposition in aridlands. This study addresses the challenges of estimating aridland inorganic N deposition using multiple methods across an urban-rural and precipitation gradient to capture long-term and seasonal patterns of wet and dry N deposition.

Most N deposition studies employ a single empirical or modeling approach to estimate wet and dry deposition over relatively short time periods. However, single approaches can lead to uncertainty under temporally and spatially heterogeneous environmental conditions common to aridlands. For example, throughfall measurements likely misrepresent deposition because leaf surfaces can become saturated with dry deposition during periods without rain and N may volatilize off surfaces before being washed into throughfall collectors (Fenn et al., 2000, 2009; Padgett et al., 2008). While wet deposition is an important seasonal input to arid systems (Báez et al., 2007; Li et al., 2013), dry deposition—much of which is expected to be dry NH_3—can contribute up to 80% of atmospheric inputs to arid landscapes between patchy storm events (Lohse et al., 2008; Fenn et al., 2010; Li et al., 2013, 2016). Dry deposition itself is challenging and costly to quantify because of the short life span of many atmospheric gases, volatilization, saturated leaf surfaces, and the bidirectional fluxes of NH_3 (Hanson and Lindberg, 1991; Lovett, 1994; Asman et al., 1998; Wesely and Hicks, 2000; Golden et al., 2008; Lohse et al., 2008; Fenn et al., 2013; Bytnerowicz et al., 2015).

Various N deposition modeling approaches also have limitations that introduce considerable uncertainty. For example, the inferential method estimates dry deposition based on deposition velocities and atmospheric concentrations of NH_3, NO_x, and nitric acid (HNO_3)—composing most of the deposited N gases (Holland et al., 2005). Deposition velocities are dependent on heterogeneous landscape characteristics, and the error in deposition velocity estimates propagate uncertainty of dry deposition (Schwede et al., 2011). Additional uncertainty arises from the bidirectional flux of NH_3, which is the difficult to quantify ecosystem-atmosphere exchange of N regulated by variable compensation points, atmospheric concentrations, canopy structure, and meteorological conditions (Asman et al., 1998; Zhang et al., 2010; Zhu et al., 2015b). Finally, N deposition estimates from regional-scale models (e.g., Community Multi-scale Air Quality (CMAQ) model) and national monitoring networks are limited in spatial resolution (e.g., 12 × 12-km; Fenn et al., 2003b; Holland et al., 2005; Bettez and Groffman, 2013; Fenn et al., 2013). In spatially heterogeneous aridland ecosystems, low-resolution models constrain the ability to examine habitat-scale deposition patterns that vary with topography and intermittent shrub cover.

In this paper, we use a unique long-term study that integrates multiple methods to address the question: what are the patterns and drivers of wet and dry inorganic N deposition in a dryland region? We assessed inorganic N deposition across a precipitation and urban-rural gradient encompassing several thousand km^2 in central Arizona in the northern Sonoran Desert. With rapid urban sprawl and over 4 million residents, the Phoenix metropolitan region and Sonoran Desert are affected by land use change, the urban heat island, and elevated reactive N gas emissions (Brazel et al., 2000; Baker et al., 2001; Grimm and Redman, 2004). Municipal ordinances have preserved large remnant patches of native Sonoran Desert arrayed along a precipitation gradient (ranging from 131 to 282 $mm\text{-}y^{-1}$; mean annual precipitation of 208-mm). This feature makes the region not only a unique study system for examining N deposition and its drivers in aridlands, but also a potentially critical carbon sink during a period of increasing anthropogenic carbon dioxide emissions (Poulter et al., 2014).

We quantified wet and/or dry inorganic N deposition continuously over 10 years (2006–2015) in the Central Arizona–Phoenix Long-Term Ecological Research (CAP LTER) study area using four different methods: co-located throughfall collectors (wet and dry deposition), bulk collectors (wet deposition), wet-dry buckets (wet and dry deposition), and passive atmospheric concentration samplers (dry deposition via inferential method). In this rapidly urbanizing area, we expected N deposition to vary spatially and seasonally, dependent on precipitation and proximity to urban activities. In particular, we predicted that the rate of inorganic N deposition would exceed the estimated desert critical load (3–9 $kgNha^{-1}y^{-1}$) with deposition primarily dominated by reduced forms of N. We also expected wet deposition patterns to follow a precipitation gradient from west to east (Table 1). Because storms are seasonal and spatially patchy, we expected the timing of rain and extended dry periods to affect the rate and form of N deposition. Thus, we predicted higher rates of wet N deposition during the semi-annual rainy seasons (i.e. associated with low-intensity winter storms and high-intensity summer monsoons) than dry seasons. However, overall, we expected dry deposition would compose the largest fraction of total annual inorganic N deposition due to long dry periods between rains.

2. Materials and methods

2.1. Wet and dry inorganic N (NH_4^++NO_3^-) deposition estimated from throughfall and bulk collectors

We measured bulk and throughfall ammonium (NH_4^+) and nitrate (NO_3^-) deposition continuously from March 2006 to June

Table 1
Characteristics of N deposition monitoring sites in remnant native desert preserves in metropolitan Phoenix, AZ (urban) and in outlying native desert to the east and west of the city.

Site Name	Elevation (m)	Annual precipitation (mm)[a]	Annual temperature (°C)[a]	Annual relative humidity (%)[a]	Annual wind speed (m/sec)[a]	Winter/summer wind direction (degrees)[a]	Housing density (house/km^2)[b]	Traffic density (cars/mile road)[b]	Agriculture (% land area)[b]
Outlying West									
Estrella Mountain East (EME)	331	154.8	24.7	28.8	1.0	170.8/189.7	37	12229	17
Estrella Mountain West (EMW)	382	147.0	24.7	28.8	1.0	170.8/189.7	7	3825	13
Sonoran National Monument East (SNE)	492	131.3	23.2	32.8	2.7	175.3/201.6	0	534	0
Sonoran National Monument West (SNW)	375	139.7	23.8	32.7	2.1	135.7/202.2	0	529	0
White Tanks Regional Park (WTM)	454	163.6	23.4	31.0	2.0	224.3/188.4	63	7428	10
Urban									
Desert Botanical Garden (DBG)	396	191.6	23.6	32.8	1.7	144.5/167.3	611	74163	8
Mountain View Park (MVP)	397	158.4	23.2	33.0	1.2	187.3/196.8	813	58308	0
Piestawa Peak (PWP)	456	167.4	23.2	33.0	1.2	187.3/196.8	631	53822	0
South Mountain East (SME)	372	159.9	23.0	30.9	1.0	150.7/195.9	395	67825	2
South Mountain West (SMW)	458	187.0	24.5	28.7	1.1	176.6/197.5	191	27542	14
Outlying East									
Lost Dutchman Park (LDP)	620	281.9	22.2	32.5	2.9	105.2/156.7	22	21271	0
McDowell Mountain North (MCN)	476	255.0	22.8	32.6	2.4	177.8/188.8	3	1662	3
McDowell Mountain South (MCS)	539	209.4	22.8	32.6	2.4	177.8/188.8	19	10915	3
Salt River Recreation area (SRR)	434	223.4	21.7	37.5	0.8	197.8/193.3	1	1936	0
Usery Mountain Park (UMP)	592	220.5	23.3	31.0	1.1	201.7/164.6	115	30264	0

[a] Annual average (2006–2015) or seasonal precipitation, temperature, relative humidity, wind speed and direction from nearest meteorological station (listed in Supplementary Material Table 1).
[b] Traffic density (2008 average weekday traffic (# vehicles)/mile of road), Housing density (2010# households/km2 from 2010 US Census Block data) and Agricultural land (% land area within buffer) calculated within 10 km buffer surrounding each site.

2015 at 15 native Sonoran Desert sites within the 6400-km^2 CAP LTER area (Fig. 1). Five monitoring sites were within remnant Sonoran Desert open space parks managed by the city ('urban', n = 5 from 2006 to 2007; n = 4 from 2007 to 2016 owing to vandalism at one site) and 5 sites each to the west and east of the city in Sonoran Desert preserves managed by Maricopa County or federal agencies ('outlying', n = 10; Table 1). All sites have sandy loam soils and similar vegetation dominated by creosotebush (*Larrea tridentata*), bursage (*Ambrosia deltoidea or A. dumosa*), succulents (*Cylindropuntia* spp, *Carnegiea gigantica*), and winter herbaceous vegetation (Hall et al., 2011; Sponseller et al., 2012).

With ion exchange resin (IER) collectors, we measured deposition as bulk (wet) deposition in the open spaces between plants and as throughfall (wet and dry) deposition under the dominant shrub, *L. tridentata*. Two duplicate bulk and throughfall collectors were deployed at each site continuously over 3-month sampling intervals (four collectors per site; approximately January–March, March–June, June–September, and September–December). Collectors were deployed an average of 89-days (35–121 days). Duplicate subsamples were averaged for each site and interval (14 sites x 38 sampling intervals, n = 532). The actual sample number for bulk (n = 494) and throughfall (n = 499) deposition varied due to missing, broken, or contaminated samples.

The IER collectors capture inorganic NH_4^+ and NO_3^- from deposition. The IER collectors retain N ions in the resin after only trace amounts of rain, as is common in arid systems (Fenn et al., 2002; Fenn and Poth, 2004). Throughfall collectors also capture dry deposition that has deposited to leaf surfaces above the sampler and is washed into the sampler by rain. We assumed bulk collectors placed in open spaces between plants capture negligible dry deposition (Erisman et al., 1994; Erisman and Draaijers, 1995; Fenn et al., 2002, 2009; Bettez and Groffman, 2013).

Bulk and throughfall IER collectors were built with a modified design following Fenn and Poth (2004) and Simkin et al. (2004). Each IER collector consisted of hydrochloric (HCl) acid-washed 12" PVC pipe filled with 60-mL Monosphere Dowex Resin (Dow Chemical Company). The resin-filled pipe was closed on the bottom with a PVC cap with 5–7 holes for drainage and glass wool to prevent resin loss. On the top, a cone-shaped plastic funnel (314-cm^2 diameter) was covered with mesh and bird spikes to prevent debris from contaminating the resin.

In the field, bulk IER collectors were installed 1.5-m aboveground in open areas without canopy cover. Throughfall IER collectors were placed under *L. tridentata* in 60-cm holes to allow for drainage during rain. At the end of sampling periods, all funnels and the *L. tridentata* branches above throughfall collectors were rinsed with 500-mL deionized (DI) water. Triplicate bulk and throughfall field blanks (caps on both ends without funnels) were deployed at one urban (DBG) and two outlying sites (WTM and LDP) and treated similarly to open collectors.

After field collection, NH_4^+ and NO_3^- ions were extracted with 200-mL 2 M potassium chloride (KCl) solution. KCl-resin slurries were shaken for one hour and then filtered through Whatman 42 filters pre-leached with 200-mL KCl. In addition, three KCl extract blanks were filtered. All KCl extracts were analyzed on a continuous flow injection Lachat QuikChem 8000 (Lachat Instruments) for NH_4^+ and NO_3^-. We did not separately analyze samples for nitrite, which may result in underestimation of oxidized N in our samples. All duplicates were averaged and concentrations and deposition rates are reported in mass of N atoms. The mean percent coefficient of variation among duplicates across all periods and locations was significantly lower in bulk samples (22% NH_4^+, 17% NO_3^-) than throughfall samples (35% NH_4^+, 26% NO_3^-). Average field blank NO_3^- and NH_4^+ concentrations (±1 SE) were 0.2 (±0.01) mgNL^{-1} and 0.6 (±0.03) mgNL^{-1} respectively, and comparable to those reported elsewhere (García-Gomez et al., 2016). On average, bulk field blanks were higher than throughfall field blank concentrations and the mass of N in the field blanks was 7% and 9% of average sample NO_3^- and NH_4^+ concentrations, respectively. The higher NH_4 concentration in field blanks is likely due to release of quaternary amine groups from the anion exchange resin beads, rather than resin contamination (Fenn and Poth, 2004). To account for this artifact and other sources of contamination, N concentrations in field blanks were subtracted from field samples for each date and

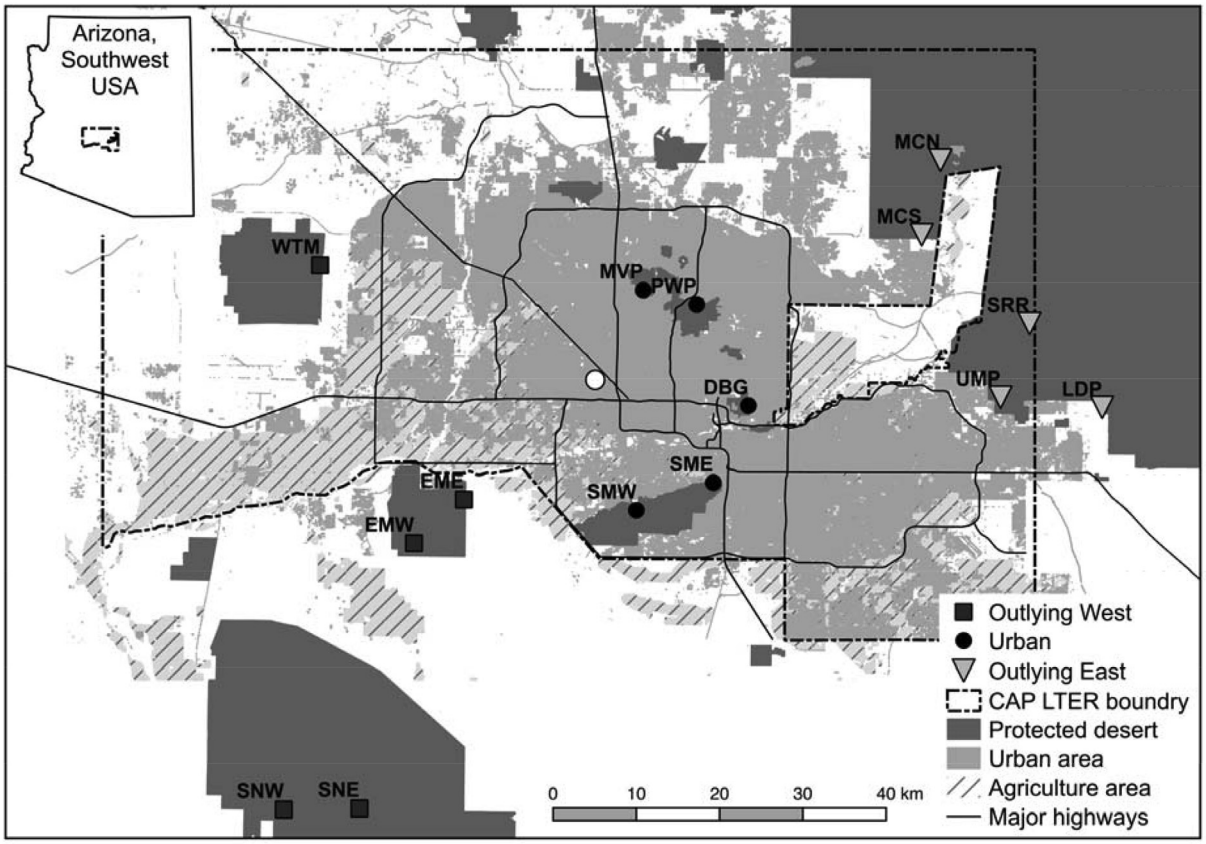

Fig. 1. N deposition monitoring sites. Long-term (2006–2015) N deposition monitoring sites within protected native desert in outlying west (square), urban (circle), and outlying east (triangle) locations in the CAP LTER study site. One urban site (open white circle) and one outlying east (LDP) site were used for monitoring atmospheric N concentrations and estimating dry N deposition in 2010–2012. Site abbreviations as in Table 1.

landscape location. Between March 2006–December 2007, there were no field blanks deployed; thus, samples from these periods were corrected with an average of field blanks from the following four sampling periods.

With corrected concentrations from KCl extracts, we calculated N deposition rates for each site using concentration in the extract ($mgNL^{-1}$), extract volume (0.2-L), funnel surface area (314-cm^2), and exposure time (days deployed in field). We present deposition in two forms as average daily deposition ($kgNha^{-1}day^{-1}$) and average yearly deposition ($kgNha^{-1}y^{-1}$). While daily and yearly rates imply a constant deposition, which is unlikely in arid systems with wet-dry pulses, this approach allows us to compare among similar periods (e.g., same season in different years) for which the exact number of sampling days differ and with previously published data.

2.2. Dry inorganic N (NO_x + NH_3+HNO_3) deposition estimated from the inferential method

We measured concentrations of gaseous NO and NO_2 (together as NO_x), NH_3, and HNO_3 using co-located passive atmospheric gas collectors. From the gaseous concentrations, we then estimated dry N deposition with the inferential method (concentration x deposition velocity; Wesely and Hicks, 2000; Fenn et al., 2009). Passive gas collectors were deployed at one urban and one outlying site (open symbol and LDP in Fig. 1) in order to compare sites with expected differences in deposition. In order to explicitly compare sampling approaches at these two sites, we deployed additional bulk and throughfall IER collectors that were co-located with the passive gas collectors. For the comparison, collectors were deployed continuously for the same intervals.

Passive gas collectors were deployed for consecutive 2- or 3-week intervals over two summer seasons (July–September 2010, July–October 2011) and two winter seasons (December 2010–March 2011, January 2011–March 2012) following established methods (Sather et al., 2008; Salem et al., 2009; Cisneros et al., 2010; Puchalski et al., 2011; Bytnerowicz et al., 2015). Ammonia, NO_x and NO_2 concentrations were measured using Ogawa Teflon passive samplers and Ogawa impregnated filter pads following previously published field and laboratory protocols (Roadman et al., 2003; Sather et al., 2007, 2008; Salem et al., 2009). Nitric acid samplers were designed following Bytnerowicz and colleagues' (2005) method using nylon membrane filters (Pall Nylasorb nylon membrane filters, 1.0-μm, 47-mm).

Passive gas collectors were transported from lab to field in individual sealed bags and plastic containers. In the field, passive collectors were installed 2-m aboveground, away from tall vegetation and structures, and under a cover to block direct sun and rain but allow air movement. At each site, we installed two NH_3 and two NO_x collectors (each holding 2 filter pads), and four HNO_3 collectors (each holding 1 filter pad). Blanks were transported to field sites but returned to the lab during the exposure period and remained sealed on a lab bench at room temperature.

At the end of each sampling interval, exposed filters were transported to the lab and transferred to 20-ml acid-washed glass vials. Dry filters were stored in a freezer up to 90 days until analysis (Ogawa, 2010). Each filter was extracted separately with DI water and shaken on a shaker table at 165-rpm for 15-min before analysis

(Bytnerowicz et al., 2005; Cisneros et al., 2010; Ogawa protocol 2010). NH_3, NO_x and NO_2 filters were extracted with 8-mL DI water and HNO_3 filters with 20-mL DI water. NH_3 and HNO_3 samples were filtered through a 0.02-μm filter (Acrodisc 13-mm, 0.2-μm nylon filter) and analyzed on a Dionex ion chromatograph (Dionex Corporation). NO_x and NO_2 filters were analyzed on the continuous flow injection Lachat Quikchem 8000. Field and extract blanks were extracted and analyzed the same as the exposed filters. Duplicate field samples were averaged by site and sampling interval and corrected with corresponding blanks.

Ammonia and NO_x concentrations were calculated following Ogawa protocols using exposure time (min), extract concentration (μgNm^{-3}) and volume, and a conversion factor including a mass transfer diffusion coefficient of each compound's sampling rate. HNO_3 concentrations were calculated using the Bytnerowicz and colleagues' (2005) calibration curve of absorbed NO_3^- when exposed to HNO_3 doses in controlled conditions (slope = 69.498 hr-m^{-3}). While overall concentrations were relatively low, we found HNO_3 concentrations (range 0.07–0.71 μgNm^{-3}) decreased with the number of sampling days ($p < 0.01$, adjusted $R^2 = 0.24$), which may lead to an underestimation of dry HNO_3 deposition for some periods. Ammonia ($p = 0.7$) and NO_x ($p = 0.9$) concentrations did not vary with number of days deployed in the field.

Using the inferential method, we calculated dry N deposition based on concentrations (μgNm^{-3}) and deposition velocities (V_d, cm-sec^{-1}) for each gaseous N species. We used deposition velocities estimated for the outlying desert site (Gonzales and Allen, 2008), which are comparable to V_d used in other arid and urban-arid systems (Supplementary Material Table 1).

2.3. Wet and dry inorganic N (NH_4^++NO_3^-) deposition estimated from a wet-dry bucket

Wet and dry N deposition were also estimated using wet-dry bucket collectors (AeroChem Metrics, Bushnell, FL). The collectors were deployed at an eastern outlying desert site (Lost Dutchman Park, LDP) from 2006 to 2015. This method captures wet deposition in rainfall in the “wet” bucket and coarse particulate dry deposition in the “dry” bucket. However, on the whole, wet-dry collectors underestimate dry deposition, especially from fine particles and gaseous compounds (Lohse et al., 2008), and are thus used here only as a lower-bound estimate. Standard methods were used in the field and lab as reported by Lohse et al. (2008). In short, rain samples were collected within 24-h of precipitation events, inspected for contamination, brought to the lab and transferred to acid washed bottles. Dry buckets were collected from the field monthly, inspected for contaminants, rinsed with 500-mL DI water, and shaken for 15-min on a shaker table. All samples were filtered with 0.7-μm Whatman glass fiber filters and analyzed for NH_4^+ and NO_3^- on the Lachat Quikchem 8000.

2.4. Meteorological and urban site characteristics as drivers of spatial and temporal variability

We collected a suite of micrometeorological and urban site characteristics to explore their relationship with N deposition patterns. Precipitation, relative humidity, and temperature were obtained from the nearest meteorological monitoring stations (<0.5–13-km to each site; FCDMC, 2015, Table 1 and Supplementary Material Table 2). In order to examine the temporal variability of precipitation, we calculated four precipitation metrics, in addition to total precipitation: 1) number of rain days per sampling interval, 2) ratio of rain days to rain-free days per sampling interval, 3) the longest number of consecutive rain-free days per interval, and 4) the antecedent dry days. Antecedent dry days were calculated as the number of consecutive dry days before the first rain event for each sampling interval.

We also calculated several anthropogenic site characteristics, including housing density and percentage of agricultural and desert land use/land cover within a 5-km buffer area around each site (Table 1; we tested different buffer sizes and found similar results for 10-km, 5-km, and 1-km buffers). The number of households in each buffer area was calculated from all Census blocks (U.S. Census, 2010) that overlapped the perimeter of the 5-km buffer (using the spatial join tool in ArcGIS 10.0). We calculated housing density (households-km^{-2}) by summing the number of households and dividing by the land area. Land-use and land-cover mapping were completed with 2010 Landsat Imagery at 30-m resolution that was classified into 15 classes (Li, 2015). The percentage of agricultural and desert land use and land cover was calculated within the 5-km buffer around each site. Traffic density was based on 2008 average weekday traffic counts, including heavy and light duty traffic on freeways and arterial roads, modeled from the TransCAD travel demand model (Maricopa Association of Governments Transportation Division). Using ArcGIS, we calculated traffic density by summing the traffic count and dividing by roadway length within each 5-km buffer (including road segments overlapping the perimeter of the buffer based on Spatial Join tool).

2.5. Data analyses

Statistical analyses were conducted using R (R Core Team, 2017). N deposition data were logarithmically or square root transformed to meet basic parametric assumptions. We used analysis of variance (ANOVA), followed by Tukey post-hoc tests with Bonferroni correction and significance $\sigma = 0.05$ (unless noted), to compare deposition rates between locations, seasons, and years. Aggregating temporal data to examine spatial patterns, we used a two-way ANOVA to compare deposition among sites and regions (outlying west, urban, and outlying east). We then aggregated across sites to compare intra- (seasonal) and inter-annual temporal differences. We repeated all tests using non-parametric Kruskall-Wallis rank sum test to confirm the parametric tests. All samples were considered independent from one another (i.e., a new, clean sampler was used each sampling interval), and thus we did not use repeated measures analyses.

We used multiple linear regression analyses to determine the main predictors of throughfall and bulk N deposition across the Phoenix metropolitan region. We calculated corrected Akaike Information Criterion (AICc) and Akaike weights with the MuMin Package in R to compare the candidate models and determine the most parsimonious model. As no one model was overwhelmingly supported (i.e., all model weights <0.5), we used model averaging to address the uncertainty in model selection (Burnham and Anderson, 2003; Johnson and Omland, 2004). We averaged model parameters for models with delta AICc less than 2.0 (Supplementary Material Table 3). We expected timing of pulsed precipitation events, meteorological factors, and site-specific characteristics to be important drivers of throughfall and bulk deposition in these aridlands. To determine the relative importance of each variable, we compared standardized beta coefficients (stß) from the averaged regression model.

3. Results

3.1. Spatial and temporal variability of N deposition rates by throughfall and bulk methods

Long-term (2006–2015) rates of mean inorganic N (NH_4^++NO_3^-) throughfall and bulk deposition across the region were 3.0 (±0.1)

and 1.7 (±0.1) kgNha^{-1}y^{-1} respectively (Table 2; Fig. 2). Throughfall deposition was nearly double bulk deposition at all sites (average throughfall:bulk deposition ratio = 1.9) indicating a significant proportion of dry deposition in throughfall samples. NH_4^+ flux was greater than that of NO_3^- in both throughfall and bulk deposition, where NH_4^+ was 67% (36–97%) of total throughfall and 53% (<1–86%) of bulk deposition (Table 2).

Averaged across sampling seasons and years, total inorganic N (NH_4^++NO_3^-) in throughfall deposition differed significantly only between three sites. The within-city site at DBG (3.7 ± 0.4 kgNha^{-1}y^{-1}) had significantly higher throughfall than the outlying eastern site at SRR (2.1 ± 0.2 kgNha^{-1}y^{-1}, $p = 0.04$) and an outlying western site at EMW (2.2 ± 0.2 kgNha^{-1}y^{-1}, $p = 0.04$, Table 2). No other sites differed in total throughfall deposition. While NH_4^+ in throughfall did not differ among sites or regions ($p = 0.06$, $p = 0.1$, respectively), NO_3^- was significantly higher at two urban sites (DBG and PWP) than at three outlying sites (EME, EMW, SRR, $p < 0.001$). Likewise, NO_3^- in throughfall was significantly higher in the urban region than outlying desert regions ($p < 0.001$; Table 2). In contrast, despite a gradient in precipitation, there were no significant differences among the 14 sites in bulk deposition (total inorganic NH_4^++NO_3^- $p = 0.2$, NO_3^- $p = 0.5$, NH_4^+ $p = 0.05$). However, regionally, bulk deposition followed the pattern of the precipitation gradient and was significantly lower to the west than in the city or outlying east region (total inorganic NH_4^++NO_3^- $p < 0.01$, NO_3^- $p = 0.03$, NH_4^+ $p < 0.01$).

Throughfall and bulk inorganic N deposition varied *intra*-annually among seasons ($p < 0.001$, $p < 0.001$ respectively, Fig. 3). Both throughfall and bulk deposition rates were highest during the summer monsoon season (June–September) and lowest between March to June, while winter (January–March) and fall (October–December) had similar intermediate deposition rates (Fig. 3). Individually, NH_4^+ and NO_3^- in both throughfall and bulk deposition followed the same seasonal patterns as total N deposition (Fig. 3). There were no interaction effects among seasons and locations (by region or site) in throughfall or bulk deposition rates (two-way ANOVAs, $p > 0.5$ for all tests). Total inorganic N throughfall deposition was significantly greater than bulk deposition in all seasons, primarily driven by greater NH_4^+ in throughfall (2 way ANOVA interaction (Throughfall/Bulk x Season), total inorganic deposition $p = 0.03$, NO_3^- $p = 0.4$, NH_4^+ $p < 0.01$, Fig. 3).

Inter-annual variation of N deposition rates was minimal. Total inorganic N (NH_4^++NO_3^-) and NH_4^+ in throughfall and bulk deposition did not vary across years, despite a range of rainfall from 118-mm (2009) to 255-mm (2010; total N $p = 0.1$, $p = 0.08$; NH_4^+ $p = 0.2$, $p = 0.08$, throughfall and bulk respectively; Fig. 2 for precipitation). In contrast, NO_3^- in throughfall was significantly greater in 2007 and 2008 than in 2009, 2010, and 2012 ($p < 0.001$). NO_3^- in bulk deposition was significantly greater in 2007 than 2009 (lowest annual rainfall; $p = 0.01$).

3.2. Spatial and temporal variability of dry N deposition rates by inferential method

Dry inorganic N (NH_3, NO_x, HNO_3) deposition estimates by the inferential method (measured seasonally 2012–2014) varied mainly by location relative to the city, but less so seasonally or among years. Summed together, dry N deposition rate (NH_3+NO_x + HNO_3) was greater in the city (6.4 ± 0.5 kgNha^{-1}y^{-1}) than in outlying native desert (1.8 ± 0.3 kgNha^{-1}y^{-1}; Fig. 4). Seasonal patterns of dry deposition were less distinct, but varied by N species (Fig. 3). HNO_3 deposition was significantly greater in the summer than winter season ($p = 0.003$), while NO_x and NH_3 did not differ by season (Fig. 3). Dry deposition from the inferential method did not vary by year (2010–2012).

3.3. Drivers of long-term throughfall and bulk N deposition

We expected timing of pulsed precipitation events, meteorological factors, and site-specific characteristics to be important drivers of throughfall and bulk deposition in these aridlands. From averaged models for both throughfall and bulk deposition, we found temperature, relative humidity, total precipitation, the number of consecutive rain free days, and housing density to be

Table 2
Inorganic N deposition. Average (+/− 1SE) deposition (NH_4^++NO_3^-, kgNha^{-1}y^{-1}) from IER throughfall, IER bulk, and wet-dry bucket collectors by site and region (2006–2015; two intervals excluded due to lab errors (Spring, 2006, Spring, 2014)). Different letters within a column indicate significantly different means among sites (abc) and regions (yz). Site abbreviations as in Table 1.

	Throughfall (wet and dry)			Bulk (wet)			Wet-dry Bucket (wet and dry)
	Total inorg N (NH_4^++NO_3^-)	NH_4^+	NO_3^-	Total inorg N (NH_4^++NO_3^-)	NH_4^+	NO_3^-	Total inorg N (NH_4^++NO_3^-)
Outlying West	**2.9 (0.2)z**	**2.1 (0.1)z**	**0.8 (0.04)z**	**1.4 (0.1)z**	**0.8 (0.1)z**	**0.6 (0.03)z**	
EME	2.5 (0.3)ab	1.8 (0.2)a	0.7 (0.1)a	1.7 (0.2)a	1.0 (0.1)a	0.7 (0.1)a	
EMW	2.2 (0.3)a	1.6 (0.2)a	0.6 (0.1)a	1.3 (0.2)a	0.8 (0.1)a	0.5 (0.1)a	
SNE	3.6 (0.5)ab	2.7 (0.4)a	0.9 (0.1)ac	1.3 (0.2)a	0.6 (0.1)a	0.6 (0.1)a	
SNW	3.5 (0.4)ab	2.6 (0.3)a	0.8 (0.1)ac	1.4 (0.2)a	0.8 (0.2)a	0.6 (0.1)a	
WTM	2.9 (0.3)ab	2.0 (0.2)a	0.9 (0.1)ac	1.5 (0.2)a	0.8 (0.1)a	0.7 (0.1)a	
Urban	**3.3 (0.2)z**	**2.3 (0.1)z**	**1.1 (0.1)y**	**1.9 (0.1)y**	**1.1 (0.1)y**	**0.8 (0.04)y**	
DBG	3.7 (0.4)b	2.5 (0.3)a	1.2 (0.1)c	1.8 (0.2)a	1.0 (0.1)a	0.7 (0.1)a	
MVP[a]							
PWP	3.5 (0.4)ab	2.2 (0.3)a	1.2 (0.1)c	1.9 (0.2)a	1.0 (0.2)a	0.8 (0.1)a	
SME	3.3 (0.4)ab	2.3 (0.3)a	0.9 (0.1)ac	2.1 (0.3)a	1.3 (0.2)a	0.8 (0.1)a	
SMW	2.9 (0.3)ab	1.9 (0.2)a	0.9 (0.1)ac	1.7 (0.2)a	1.0 (0.1)a	0.7 (0.1)a	
Outlying East	**2.7 (0.1)z**	**1.8 (0.1)z**	**0.9 (0.04)z**	**1.8 (0.1)y**	**1.1 (0.1)y**	**0.7 (0.04)yz**	
LDP	2.7 (0.3)ab	1.9 (0.2)a	0.9 (0.1)ac	2.0 (0.2)a	1.2 (0.2)a	0.7 (0.1)a	2.5 (0.2)
MCN	3.5 (0.3)ab	2.3 (0.2)a	1.2 (0.1)bc	1.8 (0.2)a	1.1 (0.1)a	0.7 (0.1)a	
MCS	2.5 (0.2)ab	1.6 (0.2)a	0.9 (0.1)ac	1.7 (0.2)a	1.0 (0.2)a	0.7 (0.1)a	
SRR	2.1 (0.2)a	1.4 (0.1)a	0.7 (0.1)ab	1.7 (0.2)a	1.1 (0.2)a	0.7 (0.1)a	
UMP	2.9 (0.3)ab	2.0 (0.2)a	0.9 (0.1)ac	1.9 (0.2)a	1.1 (0.2)a	0.8 (0.1)a	
Mean (SE) Range	**3.0 (0.1) 0.2–12.7**	**2.1 (0.1) 0.1–10.5**	**0.9 (0.03) 0.1–3.1**	**1.7 (0.1) 0.1–6.6**	**1.0 (0.04) 0.0–5.3**	**0.7 (0.02) 0.1–2.9**	

[a] Sampling limited after 2007 due to frequent vandalism and excluded from analyses.

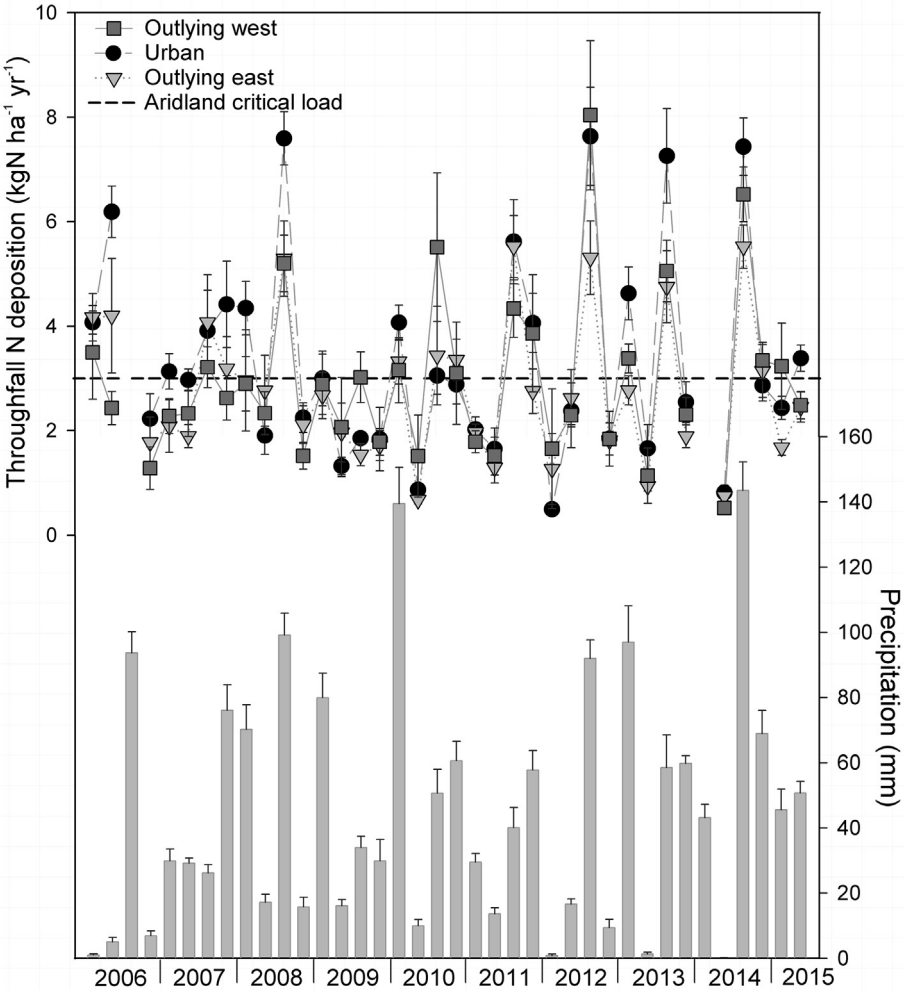

Fig. 2. Long-term seasonal N throughfall deposition and precipitation. Mean seasonal (2006–2015, ±1SE) throughfall deposition (wet and dry; NH_4^+-NO_3^-, kgNha^{-1}y^{-1}, top) and precipitation (mm, bottom). Sampling intervals approximately January–March, March–June, June–September, September–December. The lower bound of the aridland critical load (3.0 kgNha^{-1}y^{-1}) is indicated with dashed horizontal line.

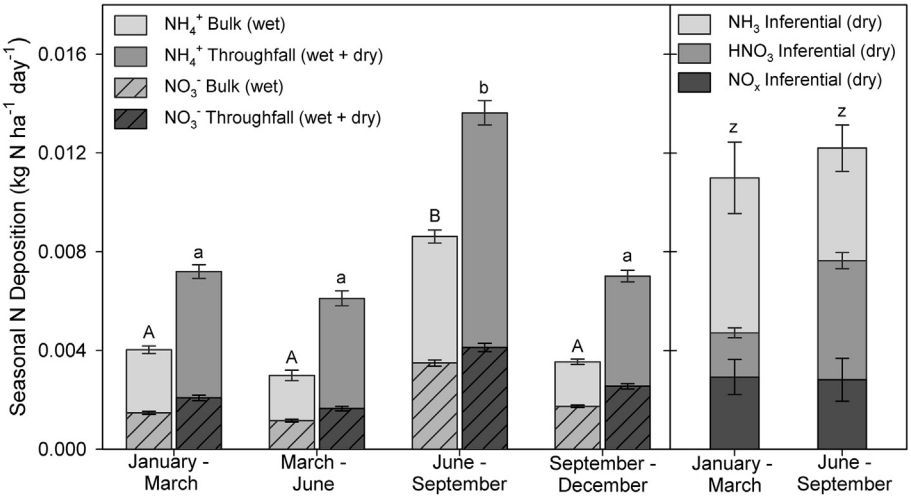

Fig. 3. Average (±1SE) seasonal inorganic NH_4^+ and NO_3^- deposition (kgNha^{-1}day^{-1}) from IER throughfall (wet and dry), IER bulk (wet), and NO_x, NH_3, and HNO_3 deposition from the passive gas collectors (inferential method, dry). Different letters indicate significantly different means of total N deposition among seasons for bulk (AB), throughfall (ab), and passive gas (zz) collectors. In addition to the statistical differences among seasons within a sampler type, throughfall was significantly greater than bulk samples in all seasons ($p < 0.01$).

important predictors. Traffic density was an additional predictor of bulk deposition. The number of days with rainfall (>5 mm) and agricultural area within a 5-km buffer were both weakly related to throughfall and bulk deposition, but were included in model averaging from models with delta AICc<2.0 (Table 3, Supplementary Material Table 2).

For throughfall, temperature (stß = +0.45), relative humidity (stß = +0.30), total precipitation (stß = +0.19), and housing density (stß = +0.15) had a positive relationship with deposition (Table 3). The number of consecutive dry days was negatively related to both throughfall and bulk deposition, where longer dry periods indicate lower rates of deposition (Table 3). The averaged model predicting bulk deposition included temperature (stß = +0.49), total precipitation (stß = +0.33), traffic density (stß = +0.31), the number of consecutive dry days (stß = −0.30), relative humidity (stß = +0.29), and housing density (stß = −0.21; Table 3).

3.4. N deposition methods comparisons

We compared total inorganic N deposition using multiple co-located sampling techniques. First, at the outlying east location, Lost Dutchman State Park (LDP), we compared wet and dry inorganic N deposition estimated with wet-dry buckets with co-located throughfall (wet and dry) and bulk (wet) IER collectors, both measured continuously from 2006 to 2015. Overall, wet and dry deposition rates were comparable among these methods and did not differ significantly by method. Average annual wet and dry deposition from wet-dry bucket collectors was 2.5 ± 0.2 compared to 2.7 ± 0.3 $kgNha^{-1}y^{-1}$ from throughfall IER collectors. Annual wet deposition was also comparable between wet bucket and bulk IER collectors (1.9 ± 0.2 and 2.0 ± 0.2 $kgNha^{-1}y^{-1}$, respectively). Average annual dry deposition collected by dry buckets at LDP, reported here as a lower bound estimate, was 0.6 ± 0.04 $kgNha^{-1}y^{-1}$. Average annual dry deposition estimated as throughfall minus bulk from co-located samplers at LDP was 0.7 ± 0.1 $kgNha^{-1}y^{-1}$. However, average annual NH_4^+ in throughfall samples (1.9 ± 0.2) was greater than NH_4^+ in wet-dry buckets (1.3 ± 0.1) and NO_3^- in throughfall was lower (0.9 ± 0.1) than NO_3^- from wet-dry buckets (1.2 ± 0.1).

Table 3
Predictors of long-term N deposition from IER throughfall (wet and dry) and bulk (wet) collectors. Predictor variables are listed in order of relative importance based on standardized coefficients. Parameter coefficients (b) and standardized coefficients (β, with confidence intervals) were averaged for all models (i.e., full average including zeros) with delta AICc<2. For individual model parameters, K, AICc, delta AICc, and weights included in the average, see Supplementary Material Table 2.

	b	St β
Throughfall (wet and dry)		
Temperature	0.0057	0.45 (0.37–0.54)
Relative humidity	0.0028	0.30 (0.18–0.42)
Number of consecutive non-rain days	−0.0010	−0.28 (−0.36–0.20)
Total precipitation	0.0004	0.19 (0.07–0.31)
Housing density	0.0001	0.15 (0.08–0.21)
Number of days with >5 mm rain	0.0017	0.05 (−0.03–0.21)
Agricultural area	−0.0006	−0.02 (−0.10–0.02)
Bulk (wet)		
Temperature	0.006001	0.49 (0.42–0.56)
Total precipitation	0.000698	0.33 (0.24–0.43)
Traffic density	0.000001	0.31 (0.17–0.46)
Number of consecutive non-rain days	−0.001058	−0.30 (−0.37–0.23)
Relative humidity	0.002704	0.29 (0.20–0.39)
Housing density	−0.000090	−0.21 (−0.35–0.06)
Agricultural area	0.001622	0.05 (0.01–0.12)
Number of days with >5 mm rain	0.000113	0.003 (−0.09–0.10)

Second, at an urban and outlying site, we compared deposition rates from throughfall samplers, which we expected to capture both wet and dry deposition, to deposition rates estimated by adding wet and dry deposition measured separately in co-located samplers (from bulk IER collectors and passive inferential dry collectors ('bulk + dry'), respectively; 2010–2012, Fig. 4). Throughfall deposition estimates were significantly lower (average of 54% lower) than deposition estimated by adding wet (bulk IER) and dry (passive inferential) deposition (paired *t*-test, $t = 4.4$, $df = 7$, $p = 0.003$; Fig. 4). However, overall variance was high. Dry deposition estimated as throughfall minus bulk deposition was only 25% of total (throughfall) deposition, whereas dry deposition estimated by inferential method composed 69% of total (bulk + dry) deposition estimated as a sum of bulk (wet) and passive inferential (dry) methods.

4. Discussion

4.1. Empirical estimates of N deposition in arid and semi-arid systems

Atmospheric nitrogen deposition has important consequences for ecosystems and plant community composition—alleviating nutrient limitation, stimulating primary production, and altering biogeochemical cycling (Aber et al., 1998; Clark and Tilman, 2008; Payne et al., 2013). However, the impacts of N deposition in aridlands, characterized by heterogeneous vegetation and patchy precipitation, likely differ from those highlighted in more temperate regions where the majority of the N deposition studies have been conducted. As urbanization in arid regions outpaces that in temperate regions, a better understanding of the spatial and temporal patterns of N deposition to aridlands is needed for determining ecosystem consequences.

Total N deposition in arid regions, and particularly dry N deposition, is commonly underestimated and necessitates multiple sampling approaches (Lohse et al., 2008; Fenn et al., 2009). Few studies have extensively examined N deposition over long periods or across urban–rural and precipitation gradients where N inputs are expected to have the most important ecological impacts. Here we used multiple sampling approaches to show a) inorganic N deposition is relatively low across both urban and outlying regions in the Sonoran Desert, b) dry deposition is an important component of total deposition, especially within the city, c) season, timing of precipitation, and proximity to sources are important drivers of N deposition patterns in this aridland ecosystem, and d) finally, despite overall low levels, deposition across the region occurs at or above the aridland critical load—the ecosystem threshold reported previously in the literature (Fenn et al., 2003a, 2010; Pardo et al., 2011; Simkin et al., 2016).

We found that inorganic N deposition rates estimated as throughfall and bulk deposition were an order of magnitude lower in Phoenix and the surrounding desert than those reported from other arid and urban areas. From 2006 to 2015, average annual wet and dry N deposition estimated as throughfall was only 3.0 $kgNha^{-1}y^{-1}$ and, contrary to expectations, showed little spatial variation across an urban–rural or precipitation gradient (Table 2, Fig. 2). These unusually low deposition estimates are corroborated by similar estimates from co-located wet and dry buckets (2.5 ± 0.2 $kgNha^{-1}y^{-1}$) in an outlying desert location (2006–2015) and a previous study in the Phoenix metropolitan region (4 $kgNha^{-1}y^{-1}$, 2000–2005; Lohse et al., 2008). Yet, short-term N deposition rates measured with similar methods in other large cities, including some semi-arid regions of the US (e.g., Los Angeles) and China (e.g., Urumqi), are at least 15 $kgNha^{-1}y^{-1}$ and often exceed 30–60 $kgNha^{-1}y^{-1}$ (Alonso et al., 2005; Rao and Allen, 2010; Cisneros

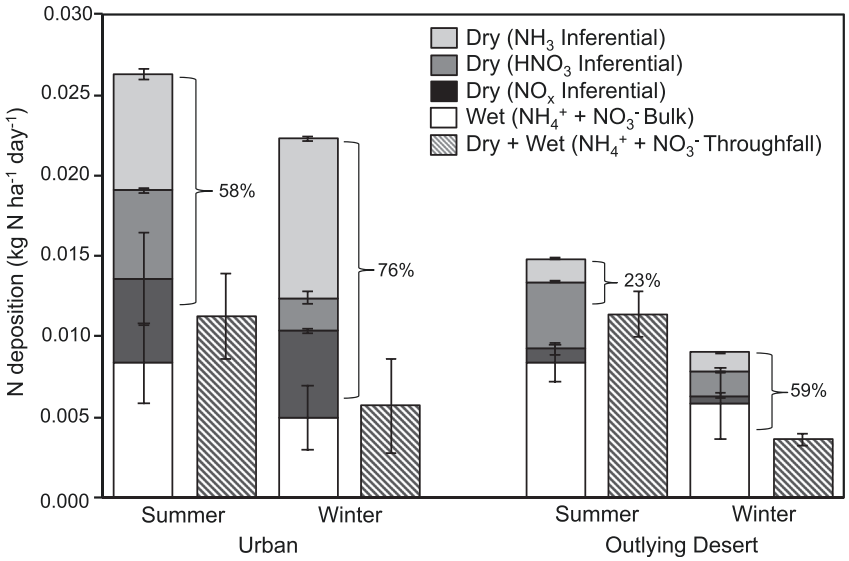

Fig. 4. Total N deposition estimates from multiple methods. N deposition ($kgNha^{-1}day^{-1}$) measured with co-located throughfall (wet and dry deposition) and bulk IER (wet deposition) collectors and passive gaseous samplers (dry deposition from inferential method) at an urban and outlying location. Stacked bars show mean N deposition (±1SE) by method between 2010 and 2012. Brackets show percent difference in total N deposition estimates by season and location; mean percent difference (across all seasons and locations) in N deposition estimates is 54%.

et al., 2010; Pan et al., 2012; Rao et al., 2013; Li et al., 2013; Bettez and Groffman, 2013; Decina et al., 2017). Higher estimates in some cities may result from specific landscape and vegetation characteristics that influence deposition velocities and leaf surface capture, proximity of sampling locations to roads and other sources of emissions, and fog—an important source of N in coastal cities (Fenn et al., 2000, 2018; Weathers et al., 2000a; Decina et al., 2017).

Lower than expected N deposition from throughfall and wet-dry buckets can be explained in part by the failure of these approaches to capture gaseous dry deposition, which is expected to be an important input to urban aridland ecosystems (Lohse et al., 2008; Fenn et al., 2010; Li et al., 2013, 2016). Dry deposition is characteristically difficult to quantify, especially in arid and semi-arid ecosystems, due to prolonged dry periods, sporadic and spatially heterogeneous rain, and plant interactions. Throughfall measurements have been reported to underestimate deposition even in temperate systems when compared with alternative sampling approaches (Weathers et al., 2000b; Fenn et al., 2013). For example, Fenn et al. (2013) found wet and dry N deposition in western US forests was underestimated using the throughfall method by 20–40%, and up to 80% during winter months, because N uptake through plant leaves reduces the dry deposition collected as throughfall. Leaf uptake or retention of N by the resinous (sticky) leaves of the dominant shrub *L. tridentata* likely contributes to throughfall underestimation in our system. Additionally, leaf saturation and volatilization of N from leaf surfaces—especially during prolonged dry periods—are also likely reasons total deposition is underestimated by throughfall measurements in aridlands. In this study, throughfall deposition, per unit time, was negatively associated with the length of dry periods (Table 3) indicating potential plant uptake or volatilization during these dry periods.

The wet-dry bucket method also underestimates dry deposition and can only be considered a minimum estimate. While the "dry" buckets may capture large particulate matter transported from downwind sources or re-suspended from the local landscape, previous studies find "dry" buckets grossly underestimate fine particulate and gaseous N (Lohse et al., 2008) and the capture of local re-deposition is minimal (Anderson and Downing, 2006). Due to these limitations, we consider wet-dry bucket deposition to be a minimum estimate of primarily external N inputs to the system. As the wet-dry bucket estimates are comparable to deposition from throughfall collectors (Table 2), the results further highlight the underestimated dry deposition in this system from throughfall (Fig. 4).

To address the uncertainties in dry deposition and sampling approaches in arid systems, we estimated gas phase N and dry N deposition with the inferential method using passive gas samplers co-located with throughfall samplers. As one of only a few such studies, we measured the dominant dry gaseous N compounds NH_3, HNO_3, and NO_x concurrently over multiple seasons in the urban and outlying desert (Zbieranowski and Aherne, 2012; Li et al., 2013). The resulting dry N deposition rate and gaseous N concentrations in the Phoenix region were at the low end, but comparable to short-term studies in other urban regions that used this method (Bytnerowicz et al., 2007; Cisneros et al., 2010; Zbieranowski and Aherne, 2012; Li et al., 2013). Only accounting for the dry component with the inferential estimate, within-city N deposition was 6.4 $kgNha^{-1}y^{-1}$—nearly double the throughfall estimate (3.3 $kgNha^{-1}y^{-1}$; Fig. 4). Unlike estimates from throughfall, dry deposition patterns highlight the urban–rural gradient in N enrichment, with 72% greater dry deposition in the city (6.4 $kgNha^{-1}y^{-1}$) than in outlying native desert (1.8 $kgNha^{-1}y^{-1}$).

4.2. Accounting for dry deposition in aridland long-term N deposition

Given inadequacies in the throughfall method for aridlands, we estimate total inorganic N deposition by comparing long-term throughfall N fluxes to an improved estimate based on the sum of wet (bulk IER collectors) and dry deposition (inferential method) measured separately. On average, throughfall estimates were lower than this improved estimate by 54% (Fig. 4). By applying this underestimation (54%) to the original long-term throughfall estimates in our study region, average regional deposition would be as high as 6.5 $kgNha^{-1}y^{-1}$, with 7.2 $kgNha^{-1}y^{-1}$ deposited in urban areas (Fig. 5).

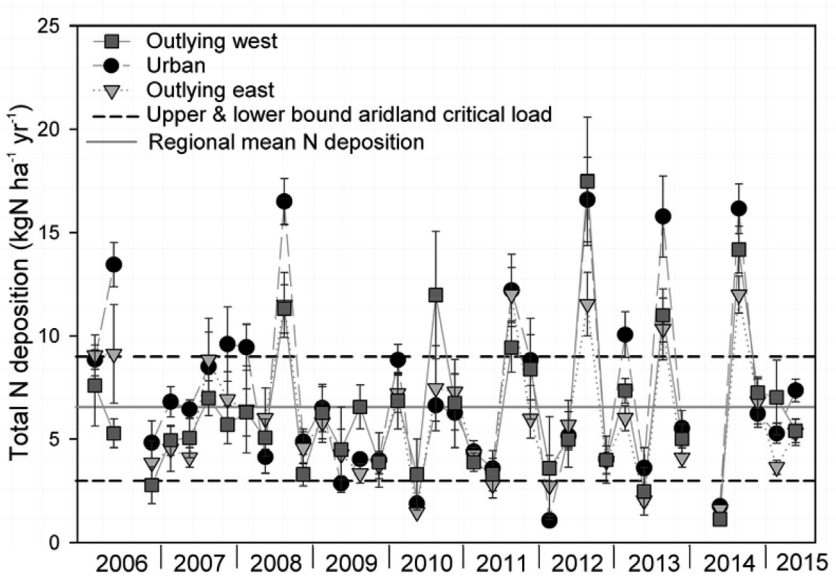

Fig. 5. Total N deposition across multiple seasons. Seasonal deposition (wet and dry, $kgNha^{-1}y^{-1}$, between January–March, March–June, June–September, and September to December) estimated for each region by accounting for the underestimation of measured throughfall. Solid line indicates mean across all sites and seasons (6.5 $kgNha^{-1}y^{-1}$) and dashed lines indicate lower (3 $kgNha^{-1}y^{-1}$) and upper (9 $kgNha^{-1}y^{-1}$) estimates for the critical load in arid ecosystems.

Even accounting for dry deposition from the inferential method, we must still consider the uncertainty in total inorganic N deposition estimates. For example, deposition velocities, which are dependent on meteorological factors and heterogeneous characteristics of the vegetation, impact deposition estimates for each N compound individually (Wesely and Hicks, 2000). The Sonoran Desert deposition velocities in this study are comparable to those applied in the other arid and urban-arid studies (Supplementary Material Table 1). However, if we applied deposition velocities used in two semi-arid cities in China (1.77-cm-s^{-1} HNO_3, 0.28-cm-s^{-1} NH_3, 0.17-cm-s^{-1} NO_2; Supplementary Material Table 1; Pan et al., 2012; Li et al., 2013), dry deposition alone in metro Phoenix would be 10.2 $kgNha^{-1}y^{-1}$ or 59% higher than our current urban estimate from the inferential method (6.4 $kgNha^{-1}y^{-1}$). On the other hand, given we were not able to account for bidirectional NH_3 fluxes, dry NH_3 estimates may represent an upper bound of dry NH_3 inputs to the system (Pan et al., 2012), which could in part account for the significant underestimation of total deposition by throughfall. Likewise, our total inorganic N deposition calculation assumes bulk collectors only captured wet deposition and no dry deposition. Previous studies apply a similar assumption, but some dry deposition in bulk collectors is inevitable and may result in 15–25% overestimation of wet deposition (Erisman and Draaijers, 1995). Both factors could account for a portion of the significant underestimation of dry deposition by throughfall.

Finally, the percent by which throughfall underestimated total inorganic N deposition will vary by landscape location, season, and proximity to emissions' sources. While the average throughfall underestimation was 54% across locations and seasons, we found substantial variation in the amount throughfall underestimated total deposition—between 23% in summer in outlying desert to 76% underestimation in the winter in an urban location (Fig. 4). The winter atmospheric inversion may allow gases to build up in the atmosphere, but limit the dry particle deposition—explaining the high gaseous concentrations captured by the passive gas samplers compared to the low dry deposition in throughfall. Despite this variability and other uncertainties, we believe the "corrected" throughfall estimates accounting explicitly for both wet and dry deposition provide a more accurate estimate of total deposition in aridlands. While each study must consider the research question and available resources (e.g., passive gas samplers require significant time and resources), we recommend deploying both bulk IER collectors and passive gas collectors across seasons and locations to estimate total deposition in aridlands.

Despite using multiple methods, our deposition rates are still lower than previously modeled estimates for the Phoenix metro area and surrounding desert (Baker et al., 2001; Fenn et al., 2003b). The regional CMAQ model (v3.0) estimated deposition to be 18–20 $kgNha^{-1}y^{-1}$ and up to 25 $kgNha^{-1}y^{-1}$ in desert areas east of Phoenix (Fenn et al., 2003b). These rates are not only much higher than our field estimates, but the CMAQ model also misidentifies hot spots of deposition across the large airshed. The higher N deposition estimates from CMAQ come from an early model (v3.0) that did not yet incorporate diurnal or bidirectional fluxes of NH_3, which have reduced error and improved deposition estimates in more recent versions (Bash et al., 2013; Zhang et al., 2010; Zhu et al., 2015b). However, regional models often overestimate N deposition at the local scale due to the coarse spatial resolution that aggregates context-specific details (Bettez and Groffman, 2013; Butler et al., 2014). The CMAQ model, on the other hand, incorporates all forms of deposition, including particulate, aerosol and gas-phase N, which we were not able to include in our estimates. Specifically, we did not account for inputs of dissolved organic nitrogen (DON), although we expect DON to be a minimal contribution to the total N deposition flux in arid regions (Neff et al., 2002; Cornell, 2011; Zhu et al., 2015a).

Additional uncertainties in empirical estimates of N deposition, especially in aridland and urban regions, result from the difficulty in accounting for seasonal and diurnal atmospheric mixing patterns, complex topography, patchy precipitation patterns, and leaf surface interactions (Nunnermacker et al., 2004; Wang and Ostoja-Starzewski, 2004; Lee et al., 2007; Lohse et al., 2008). These are areas for future research. For example, the unstable summer atmosphere can cause significant mixing and deposition of gaseous particles, while the more stable winter inversion limits the vertical flux of gaseous particles and allows NO_x and NH_3 in gaseous forms to build up in the city atmosphere and impact the bidirectional flux of NH_3. Additionally, the urban topography (i.e., building height)

likely impacts mixing and deposition patterns. Finally, passive deposition collection methods, including throughfall collectors and passive gaseous samplers, have a low temporal resolution (2 weeks–3 months). Thus, it is difficult to connect N deposition to temporally variable rainfall, meteorological factors, and ecosystem interactions (Golden et al., 2008). Short-term processes of leaf saturation, biological uptake, bidirectional fluxes of NH_3, or volatilization of deposition collected on leaf surfaces during hot periods magnify the uncertainty of empirical deposition estimates (Wesely and Hicks, 2000).

4.3. Timing and frequency of precipitation and proximity to sources affect aridland N deposition

Despite the lower than anticipated dry component from throughfall approaches, the extensive spatial and continuous long-term sampling provide important insight into the patterns and drivers of N deposition in the region across seasons and years of above average and below average precipitation. The amount of precipitation is an important driver of deposition (Table 3). Yet, the Sonoran Desert is characterized by bimodal precipitation, with distinct rain seasons in winter and summer (Báez et al., 2007; Lohse et al., 2008). Despite similar amounts of precipitation, summer throughfall deposition estimates (0.014 $kgNha^{-1}day^{-1}$) were double those in the winter (0.007 $kgNha^{-1}day^{-1}$; Fig. 2; Fig. 3). These findings suggest that total seasonal rainfall is not the main driver of N deposition in arid systems, as was expected, but that other seasonally changing factors also influence deposition.

In addition to total precipitation, we found summer meteorological and storm patterns, including temperature and the timing and frequency of precipitation, influence rates of summer N deposition. Summer dust and lightning storms are sources of increased particulate matter and atmospheric NO_x, respectively (Nickling and Brazel, 1984; Schumann and Huntrieser, 2007). Likewise, the summer monsoon season brings heavy precipitation and relative humidity, which are favorable conditions for aerosol formation of highly soluble NO_3^- and NH_4^+ that deposit close to their sources. Higher N deposition in throughfall occurred during periods with more frequent rainfall, higher relative humidity, and higher temperatures during summer monsoon seasons. In contrast, longer dry periods without rain had lower deposition rates (Table 3). These trends lend support to the hypothesis that deposition, in particular the dry component, may be underestimated during long dry periods by throughfall methods when 1) leaf surfaces become saturated prohibiting further collection of N deposition on the surface of leaves or 2) particulate N volatilizes from leaf surfaces during hot periods.

In addition to seasonal patterns, the spatial distribution of NH_4^+ and NO_3^- (and their various gaseous components) in deposition is an important indicator of the source of deposition (Holland et al., 2005; Li et al., 2013; Rao et al., 2013). In general, high NH_4^+:NO_3^- in deposition suggests the importance of agricultural sources (N fertilizer applications and animal husbandry). Lower NH_4^+:NO_3^- ratios indicate sources of NO_x from industrial combustion and vehicular emissions that are deposited as NO_3^- in precipitation. Recent trends across the continent show higher NH_4^+:NO_3^- as N emissions in the US shifted from oxidized N to predominantly reduced N as a result of policies that limit industrial NO_x emissions (Ellis et al., 2013). These patterns have not been well studied at local scales near sources, or across seasons where temperature and precipitation patterns can have a large impact on deposition.

Following national trends, we found spatial and temporal differences in NH_4^+:NO_3^-. Vehicular and industrial influence on N deposition is stronger in the city (urban throughfall NH_4^+:$NO_3^- = 2.1$) than in the outlying region (outlying throughfall NH_4^+: $NO_3^- = 2.7$) with extensive agricultural land west of the city (Table 1; Lovett et al., 2000; Holland et al., 2005; Pan et al., 2012; Rao et al., 2013; Li et al., 2013; Bettez and Groffman, 2013). As in other cities, gaseous NO_x concentrations are an important component of the urban atmosphere (Sather et al., 2007; Moodley et al., 2011; Li et al., 2013) where housing and traffic density were important drivers of long-term throughfall and bulk deposition, respectively (Table 3). However, we expect the oxidized N emissions from vehicles would have been an even greater impact on NH_4^+:NO_3^-, as well as stronger predictor of deposition, if sampling had occurred closer to major roadways where N fluxes have been reported up to 4 times higher than more remote sites (Redling et al., 2013; Decina et al., 2017). Our urban study sites located within remnant protected desert parks may not capture this variability in oxidized N from roadside emissions. Recent research also suggests that while agriculture is the predominant source of NH_3 emissions, on-road NH_3 vehicle emissions may be increasingly an important contribution to high NH_4^+:NO_3^- in urban regions (Bishop and Stedman, 2015; Sun et al., 2017; Decina et al., 2017; Fenn et al., 2018). Overall, the high regional NH_4^+:NO_3^- in long-term throughfall deposition (average 2.3) with 67% NH_4^+ highlights the strong contribution of agricultural emissions throughout the region.

Li et al. (2016) recently observed that a significant proportion of total N deposition (79%) is deposited as dry NH_3 in the US Southwest, including Arizona and California. Consistent with this, we found NH_3 was the most significant component of dry N deposition in the city (average 41%) and HNO_3 was important in outlying regions (Fig. 4; Cisneros et al., 2010; Pan et al., 2012). Higher NH_4^+ deposition—especially in the summer (Fig. 3)—is likely influenced by increased coarse particulate material from frequent dust storms and high rates of NH_3 volatilization from alkaline agricultural and native desert soils (McCalley and Sparks, 2008). Overall, our results highlight that stricter restrictions on agricultural NH_3 emissions will be necessary to limit future regional N deposition and protect native landscapes.

4.4. Potential ecosystem consequences of aridland N deposition

While lower than other arid urban regions, the total N deposition rate in this aridland ecosystem is at the upper limit of the expected aridland ecological threshold, or N critical load (Fig. 5; 3–9 $kgNha^{-1}y^{-1}$; Fenn et al., 2010; Pardo et al., 2011). N deposition in the Sonoran Desert, even at a relatively low rate, is likely to have significant ecological impacts particularly when water is less limiting to biotic processes during the rainy seasons. For example, one study reported lower rates of N deposition to aridlands likely disrupt biotic and abiotic ecosystem interactions more than higher rates of deposition (i.e. ~10-$kgNha^{-1}y^{-1}$ compared to 30–50 $kgNha^{-1}y^{-1}$; Ochoa-Hueso, 2016). Likewise, Simkin et al. (2016) report that deposition rates above 8.8 $kgNha^{-1}y^{-1}$ were associated with declining herbaceous species richness in grasslands and shrublands with alkaline soils similar to our Sonoran Desert study sites (Hall et al., 2011).

Moreover, ecosystem responses to N enrichment are context dependent and vary seasonally and spatially depending on temperature and precipitation (Simkin et al., 2016). Despite low deposition compared to other arid and urban regions, elevated rates during the early winter growing season (Fig. 3) are likely to influence aridland ecosystem structure and function, particularly in rainy years and seasons when water limitation is alleviated and microbial and herbaceous plant communities are more active (Shen et al., 2008; Hall et al., 2011). While shrub growth may be insensitive to N inputs (Hall et al., 2011), higher deposition captured as throughfall under shrubs augments herbaceous and microbial growth, contributing to 'islands of fertility' in desert ecosystems (Schade and Hobbie, 2005; McCrackin et al., 2008; Hall et al., 2011;

Tulloss and Cadenasso, 2015). Following a long period of N accumulation on leaf and soil surfaces, a pulse of rain can stimulate biological responses and biogeochemical transformations of deposited NH_4^+ and NO_3^-, which can then be redistributed in the ecosystem (Belnap et al., 2005; Welter et al., 2005; Hall et al., 2011). These islands of fertility will contribute to the significant carbon sink in heterogeneous aridlands (Poulter et al., 2014). Thus, chronic, long-term deposition, even at the low end of the critical load, can have significant effects on ecosystems and community composition, including increased annual herbaceous plant growth and a loss of native desert species diversity (Brooks, 2003; Báez et al., 2007; Rao et al., 2010).

5. Conclusion

While aridlands cover a third of Earth's terrestrial surface and are likely to incur increased human activities and N deposition, the long-term rates of atmospheric N inputs in aridlands have been relatively unstudied. Here, we quantified spatial and temporal patterns of inorganic N deposition in protected aridlands across an extensive urban-rural and precipitation gradient using multiple sampling methods. From IER collectors and passive samplers with the inferential method, we determined that 7.2 ± 0.4 kgNha^{-1}y^{-1} is deposited to protected Sonoran Desert lands within the urban boundaries of metro Phoenix and an average of 6.5 ± 0.2 kgNha^{-1}y^{-1} across the region (Fig. 5). Across all locations, deposition rates are even higher during the summer season. Regardless of season or location, deposition rates are within or exceed the range of the aridland critical load (3–9 kgNha^{-1}y^{-1}) at which ecological consequences are expected to occur.

Our approach highlights the importance of mixed methods to strengthen estimates of total inorganic N deposition in heterogeneous aridland systems. Regional scale models overestimated deposition rates for our sampling period by 60% and misidentified hot spots of deposition across the airshed. By contrast, the easily deployed throughfall IER collectors underestimated deposition fluxes (mostly dry deposition) by 54% and showed minimal spatial variation across the urban–rural gradient. However, seasonal sampling of the IER collectors over 10 years allowed us to capture seasonal variation in atmospheric N inputs connected to the timing of precipitation. From our comparison of methods, we recommend that throughfall collectors be used with caution to estimate total inorganic N deposition, particularly dry deposition, to arid systems. Co-locating bulk IER collectors to capture wet deposition with passive samplers and inferential methods to capture dry deposition can be a good alternative. However, the best method(s) will depend on the context, research question, resources available, and associated uncertainties of each method. Our results, derived from the longest, spatially and temporally explicit dataset in aridlands to date, highlight the importance of long-term, mixed approaches to estimate atmospheric nutrient enrichment to arid and semi-arid ecosystems in a rapidly changing world.

Acknowledgements

We thank Diane Alexander, Stevan Earl, Roy Erickson, Kris Fecteau, David Huber, Cathy Kochert, Jennifer Learned, Yevgeniy Marusenko, Sam Norlin, Brenda Ramierz, Michelle Schmoker Davis, and Quincy Stewart for help with field and laboratory work; Ron Pope for providing local traffic data; and Daniel Henz for providing meteorological data. This work was work supported by the National Science Foundation under grant no. DEB-0423704, BCS-1026865, and DEB-1637590 Central Arizona–Phoenix Long-term Ecological Research program and grant no. 0504248, Integrative Graduate Education Research and Training (IGERT) in Urban Ecology.

Appendix A. Supplementary data

Supplementary data related to this article can be found at https://doi.org/10.1016/j.envpol.2018.04.013.

References

Aber, J.D., McDowell, W., Nadelhoffer, K., Magill, A., Berntson, G., Kamakea, M., McNulty, S., Currie, W., Rustad, L., Fernandez, I., 1998. Nitrogen saturation in temperate forests: hypotheses revisited. Bioscience 48, 921–934.

Aber, J.D., Ollinger, S.V., Driscoll, C.T., Likens, G.E., Holmes, R.T., Freuder, R.J., Goodale, C.L., 2002. Inorganic nitrogen losses from a forested ecosystem in response to physical, chemical, biotic,and climatic perturbations. Ecosystems 5, 0648–0658. https://doi.org/10.1007/s10021-002-0203-8.

Alonso, R., Bytnerowicz, A., Boarman, W.I., 2005. Atmospheric dry deposition in the vicinity of the Salton Sea, California—I: air pollution and deposition in a desert environment. Atmos. Environ. 39, 4671–4679. https://doi.org/10.1016/j.atmosenv.2005.04.016.

Anderson, K.A., Downing, J.A., 2006. Dry and wet atmospheric deposition of nitrogen phosphorus and silicon in an agricultural region. Water. Air. Soil Pollut. 176, 351–374. https://doi.org/10.1007/s 11270-006-9172-4.

Asman, W. a. H., Sutton, M.A., Schjørring, J.K., 1998. Ammonia: emission, atmospheric transport and deposition. New Phytol. 139, 27–48. https://doi.org/10.1046/j.1469-8137.1998.00180.x.

Báez, S., Fargione, J., Moore, D.I., Collins, S.L., Gosz, J.R., 2007. Atmospheric nitrogen deposition in the northern Chihuahuan desert: temporal trends and potential consequences. J. Arid. Environ. 68, 640–651. https://doi.org/10.1016/j.jaridenv.2006.06.011.

Baker, L.A., Hope, D., Xu, Y., Edmonds, J., Lauver, L., 2001. Nitrogen balance for the Central Arizona–Phoenix (CAP) ecosystem. Ecosystems 4, 582–602. https://doi.org/10.1007/s10021-001-0031-2.

Bash, J.O., Cooter, E.J., Dennis, R.L., Walker, J.T., Pleim, J.E., 2013. Evaluation of a regional air-quality model with bidirectional NH_3 exchange coupled to an agroecosystem model. Biogeosciences 10, 1635–1645.

Belnap, J., Welter, J.R., Grimm, N.B., Barger, N., Ludwig, J.A., 2005. Linkages between microbial and hydrologic processes in arid and semiarid watersheds. Ecology 86, 298–307. https://doi.org/10.2307/3450948.

Bettez, N.D., Groffman, P.M., 2013. Nitrogen deposition in and near an urban ecosystem. Environ. Sci. Technol. 47, 6047–6051. https://doi.org/10.1021/es400664b.

Bishop, G.A., Stedman, D.H., 2015. Reactive nitrogen species emission trends in three light-/medium-duty United States fleets. Environ. Sci. Technol. 49, 11234–11240. https://doi.org/10.1021/acs.est.5b02392.

Brazel, A., Selover, N., Vose, R., Heisler, G., 2000. The tale of two climates - Baltimore and Phoenix urban LTER sites. Clim. Res. 15, 123–135. https://doi.org/10.3354/cr015123.

Brooks, M.L., 2003. Effects of increased soil nitrogen on the dominance of alien annual plants in the Mojave Desert. J. Appl. Ecol. 40, 344–353. https://doi.org/10.1046/j.1365-2664.2003.00789.x.

Burnham, K.P., Anderson, D.R., 2003. Model Selection and Multimodel Inference: a Practical Information-Theoretic Approach. Springer Science & Business Media.

Butler, T., Marino, R., Schwede, D., Howarth, R., Sparks, J., Sparks, K., 2014. Atmospheric ammonia measurements at low concentration sites in the northeastern USA: implications for total nitrogen deposition and comparison with CMAQ estimates. Biogeochemistry 122, 191–210. https://doi.org/10.1007/s10533-014-0036-5.

Bytnerowicz, A., Johnson, R.F., Zhang, L., Jenerette, G.D., Fenn, M.E., Schilling, S.L., Gonzalez-Fernandez, I., 2015. An empirical inferential method of estimating nitrogen deposition to Mediterranean-type ecosystems: the San Bernardino mountains case study. Environ. Pollut. 203, 69–88. https://doi.org/10.1016/j.envpol.2015.03.028.

Bytnerowicz, A., Omasa, K., Paoletti, E., 2007. Integrated effects of air pollution and climate change on forests: a northern hemisphere perspective. Environ. Pollut. 147, 438–445. https://doi.org/10.1016/j.envpol.2006.08.028.

Bytnerowicz, A., Sanz, M.J., Arbaugh, M.J., Padgett, P.E., Jones, D.P., Davila, A., 2005. Passive sampler for monitoring ambient nitric acid (HNO_3) and nitrous acid (HNO_2) concentrations. Atmos. Environ. 39, 2655–2660. https://doi.org/10.1016/j.atmosenv.2005.01.018.

Cisneros, R., Bytnerowicz, A., Schweizer, D., Zhong, S., Traina, S., Bennett, D.H., 2010. Ozone, nitric acid, and ammonia air pollution is unhealthy for people and ecosystems in southern Sierra Nevada, California. Environ. Pollut. 158, 3261–3271. https://doi.org/10.1016/j.envpol.2010.07.025.

Clark, C.M., Tilman, D., 2008. Loss of plant species after chronic low-level nitrogen deposition to prairie grasslands. Nature 451, 712–715. https://doi.org/10.1038/nature06503.

Collins, S.L., Belnap, J., Grimm, N.B., Rudgers, J.A., Dahm, C.N., D'Odorico, P., Litvak, M., Natvig, D.O., Peters, D.C., Pockman, W.T., et al., 2014. A multiscale, hierarchical model of pulse dynamics in arid-land ecosystems. Annu. Rev. Ecol. Evol. Syst. 45, 397–419.

Cornell, S.E., 2011. Atmospheric nitrogen deposition: revisiting the question of the importance of the organic component. Environ. Pollut. 159, 2214–2222. https://doi.org/10.1016/j.envpol.2010.11.014.

Decina, S.M., Templer, P.H., Hutyra, L.R., Gately, C.K., Rao, P., 2017. Variability, drivers, and effects of atmospheric nitrogen inputs across an urban area: emerging patterns among human activities, the atmosphere, and soils. Sci. Total Environ.

609, 1524–1534. https://doi.org/10.1016/j.scitotenv.2017.07.166.
Dentener, F., Drevet, J., Lamarque, J.F., Bey, I., Eickhout, B., Fiore, A.M., Hauglustaine, D., Horowitz, L.W., Krol, M., Kulshrestha, U.C., Lawrence, M., Galy-Lacaux, C., Rast, S., Shindell, D., Stevenson, D., Van Noije, T., Atherton, C., Bell, N., Bergman, D., Butler, T., Cofala, J., Collins, B., Doherty, R., Ellingsen, K., Galloway, J., Gauss, M., Montanaro, V., Müller, J.F., Pitari, G., Rodriguez, J., Sanderson, M., Solmon, F., Strahan, S., Schultz, M., Sudo, K., Szopa, S., Wild, O., 2006. Nitrogen and sulfur deposition on regional and global scales: a multimodel evaluation. Glob. Biogeochem. Cycles 20. GB4003. https://doi.org/10.1029/2005GB002672.
Du, E., de Vries, W., Galloway, J.N., Hu, X., Fang, J., 2014. Changes in wet nitrogen deposition in the United States between 1985 and 2012. Environ. Res. Lett. 9, 095004. https://doi.org/10.1088/1748-9326/9/9/095004.
Ellis, R.A., Jacob, D.J., Sulprizio, M.P., Zhang, L., Holmes, C.D., Schichtel, B.A., Blett, T., Porter, E., Pardo, L.H., Lynch, J.A., 2013. Present and future nitrogen deposition to national parks in the United States: critical load exceedances. Atmos. Chem. Phys. 13, 9083–9095. https://doi.org/10.5194/acp-13-9083-2013.
Erisman, J.W., Beier, C., Draaijers, G., Lindberg, S., 1994. Review of deposition monitoring methods. Tellus B 46, 79–93.
Erisman, J.W., Draaijers, G.P.J., 1995. Atmospheric deposition. In: Relation to Acidification and Eutrophication. Elsevier.
Fenn, M.E., Allen, E.B., Weiss, S.B., Jovan, S., Geiser, L.H., Tonnesen, G.S., Johnson, R.F., Rao, L.E., Gimeno, B.S., Yuan, F., Meixner, T., Bytnerowicz, A., 2010. Nitrogen critical loads and management alternatives for N-impacted ecosystems in California. J. Environ. Manage 91, 2404–2423. https://doi.org/10.1016/j.jenvman.2010.07.034.
Fenn, M.E., Baron, J.S., Allen, E.B., Rueth, H.M., Nydick, K.R., Geiser, L., Bowman, W.D., Sickman, J.O., Meixner, T., Johnson, D.W., Neitlch, P., 2003a. Ecological effects of nitrogen deposition in the western United States. BioScience 53, 404–420. https://doi.org/10.1641/0006-3568(2003)053[0404:EEONDI]2.0.CO;2.
Fenn, M.E., Bytnerowicz, A., Schilling, S.L., Vallano, D.M., Zavaleta, E.S., Weiss, S.B., Morozumi, C., Geiser, L.H., Hanks, K., 2018. On-road emissions of ammonia: an underappreciated source of atmospheric nitrogen deposition. Sci. Total Environ. 625, 909–919. https://doi.org/10.1016/j.scitotenv.2017.12.313.
Fenn, M.E., Haeuber, R., Tonnesen, G.S., Baron, J.S., Grossman-Clarke, S., Hope, D., Jaffe, D.A., Copeland, S., Geiser, L., Rueth, H.M., 2003b. Nitrogen emissions, deposition, and monitoring in the western United States. BioScience 53, 391–403.
Fenn, M.E., Poth, M.A., 2004. Monitoring nitrogen deposition in throughfall using ion exchange resin columns. J. Environ. Qual. 33, 2007. https://doi.org/10.2134/jeq2004.2007.
Fenn, M.E., Poth, M.A., Arbaugh, M.J., 2002. A throughfall collection method using mixed bed ion exchange resin columns. Sci. World J. https://doi.org/10.1100/tsw.2002.84.
Fenn, M.E., Poth, M.A., Schilling, S.L., Grainger, D.B., 2000. Throughfall and fog deposition of nitrogen and sulfur at an N-limited and N-saturated site in the San Bernardino Mountains, southern California. Can. J. For. Res. 30, 1476–1488. https://doi.org/10.1139/x00-076.
Fenn, M.E., Ross, C.S., Schilling, S.L., Baccus, W.D., Larrabee, M.A., Lofgren, R.A., 2013. Atmospheric deposition of nitrogen and sulfur and preferential canopy consumption of nitrate in forests of the Pacific Northwest, USA. For. Ecol. Manag. 302, 240–253. https://doi.org/10.1016/j.foreco.2013.03.042.
Fenn, M.E., Sickman, J.O., Bytnerowicz, A., Clow, D.W., Molotch, N.P., Pleim, J.E., Tonnesen, G.S., Weathers, K.C., Padgett, P.E., Campbell, D.H., 2009. Chapter 8 methods for measuring atmospheric nitrogen deposition inputs in arid and montane ecosystems of western North America. In: Legge, A.H. (Ed.), Developments in Environmental Science, Air Quality and Ecological Impacts: Relating Sources to Effects. Elsevier, pp. 179–228.
Galloway, J.N., Dentener, F.J., Capone, D.G., Boyer, E.W., Howarth, R.W., Seitzinger, S.P., Asner, G.P., Cleveland, C.C., Green, P.A., Holland, E.A., 2004. Nitrogen cycles: past, present, and future. Biogeochemistry 70, 153–226.
García-Gomez, H., Izquieta-Rojano, S., Aguillaume, L., González-Fernández, I., Valiño, F., Elustondo, D., Santamaría, J.M., Àvila, A., Fenn, M.E., Alonso, R., 2016. Atmospheric deposition of inorganic nitrogen in Spanish forests of Quercus ilex measured with ion-exchange resins and conventional collectors. Environ. Pollut. 216, 653–661. https://doi.org/10.1016/j.envpol.2016.06.027.
Golden, H.E., Boyer, E.W., Brown, M.G., Elliott, E.M., Lee, D.K., 2008. Simple approaches for measuring dry atmospheric nitrogen deposition to watersheds. Water Resour. Res. 44. W00D02. https://doi.org/10.1029/2008WR006952.
Gonzales, D., Allen, J., 2008. Atmospheric deposition sampling across an urban gradient, using passive resin collectors. CAP LTER Data Cat. https://sustainability.asu.edu/caplter/data/data-catalog/view/knb-lter-cap.393.6/.
Grimm, N.B., Redman, C.L., 2004. Approaches to the study of urban ecosystems: the case of Central Arizona—Phoenix. Urban Ecosyst. 7, 199–213. https://doi.org/10.1023/B:UECO.0000044036.59953.a1.
Hall, S.J., Sponseller, R.A., Grimm, N.B., Huber, D., Kaye, J.P., Clark, C., Collins, S.L., 2011. Ecosystem response to nutrient enrichment across an urban airshed in the Sonoran Desert. Ecol. Appl. 21, 640–660. https://doi.org/10.1890/10-0758.1.
Hanson, P.J., Lindberg, S.E., 1991. Dry deposition of reactive nitrogen compounds: a review of leaf, canopy and non-foliar measurements. Atmos. Environ. Part Gen. Top. 25, 1615–1634. https://doi.org/10.1016/0960-1686(91)90020-8.
Holland, E.A., Braswell, B.H., Sulzman, J., Lamarque, J.-F., 2005. Nitrogen deposition onto the United States and western Europe: synthesis of observations and models. Ecol. Appl. 15, 38–57. https://doi.org/10.1890/03-5162.
Johnson, J.B., Omland, K.S., 2004. Model selection in ecology and evolution. Trends Ecol. Evol. 19, 101–108.
Ladwig, L.M., Collins, S.L., Swann, A.L., Xia, Y., Allen, M.F., Allen, E.B., 2012. Above- and belowground responses to nitrogen addition in a Chihuahuan Desert grassland. Oecologia 169, 177–185. https://doi.org/10.1007/s00442-011-2173-z.
Lee, S.-M., Fernando, H.J.S., Grossman-Clarke, S., 2007. MM5-SMOKE-CMAQ as a modeling tool for 8-h ozone regulatory enforcement: application to the state of Arizona. Environ. Model. Assess. 12, 63–74. https://doi.org/10.1007/s10666-006-9053-7.
Li, K., Liu, X., Song, W., Chang, Y., Hu, Y., Tian, C., 2013. Atmospheric nitrogen deposition at two sites in an arid environment of central Asia. PLoS One 8 e67018. https://doi.org/10.1371/journal.pone.0067018.
Li, X., 2015. Land use and land cover (LULC) classification of the CAP LTER study area using 2010 Landsat imagery. CAP LTER Data Cat. https://sustainability.asu.edu/caplter/data/data-catalog/view/knb-lter-cap.619/.
Li, Y., Schichtel, B.A., Walker, J.T., Schwede, D.B., Chen, X., Lehmann, C.M.B., Puchalski, M.A., Gay, D.A., Collett, J.L., 2016. Increasing importance of deposition of reduced nitrogen in the United States. Proc. Natl. Acad. Sci. 113, 5874–5879. https://doi.org/10.1073/pnas.1525736113.
Lloret, J., Valiela, I., 2016. Unprecedented decrease in deposition of nitrogen oxides over North America: the relative effects of emission controls and prevailing air-mass trajectories. Biogeochemistry 1–2, 165–180. https://doi.org/10.1007/s10533-016-0225-5.
Lohse, K.A., Hope, D., Sponseller, R., Allen, J.O., Grimm, N.B., 2008. Atmospheric deposition of carbon and nutrients across an arid metropolitan area. Sci. Total Environ. 402, 95–105. https://doi.org/10.1016/j.scitotenv.2008.04.044.
Lovett, G.M., 2013. Critical issues for critical loads. Proc. Natl. Acad. Sci. 110, 808–809. https://doi.org/10.1073/pnas.1219007110.
Lovett, G.M., 1994. Atmospheric deposition of nutrients and pollutants in North America: an ecological perspective. Ecol. Appl. 4, 629–650.
Lovett, G.M., Traynor, M.M., Pouyat, R.V., Carreiro, M.M., Zhu, W.-X., Baxter, J.W., 2000. Atmospheric deposition to oak forests along an urban-rural gradient. Environ. Sci. Technol. 34, 4294–4300.
McCalley, C.K., Sparks, J.P., 2008. Controls over nitric oxide and ammonia emissions from Mojave Desert soils. Oecologia 156, 871–881. https://doi.org/10.1007/s00442-008-1031-0.
McCrackin, M.L., Harms, T.K., Grimm, N.B., Hall, S.J., Kaye, J.P., 2008. Responses of soil microorganisms to resource availability in urban, desert soils. Biogeochemistry 87, 143–155. https://doi.org/10.1007/s10533-007-9173-4.
Moodley, K.G., Singh, S., Govender, S., 2011. Passive monitoring of nitrogen dioxide in urban air: a case study of Durban metropolis, South Africa. J. Environ. Manage 92, 2145–2150. https://doi.org/10.1016/j.jenvman.2011.03.040.
Neff, J.C., Holland, E.A., Dentener, F.J., McDowell, W.H., Russell, K.M., 2002. The origin, composition and rates of organic nitrogen deposition: a missing piece of the nitrogen cycle? Biogeochemistry 57, 99–136.
Nickling, W.G., Brazel, A.J., 1984. Temporal and spatial characteristics of Arizona dust storms (1965–1980). J. Climatol. 4, 645–660. https://doi.org/10.1002/joc.3370040608.
Noy-Meir, I., 1973. Desert ecosystems: environment and producers. Annu. Rev. Ecol. Syst. 4, 25–51. https://doi.org/10.1146/annurev.es.04.110173.000325.
Nunnermacker, L.J., Weinstein-Lloyd, J., Kleinman, L., Daum, P.H., Lee, Y.N., Springston, S.R., Klotz, P., Newman, L., Neuroth, G., Hyde, P., 2004. Ground-based and aircraft measurements of trace gases in Phoenix, Arizona (1998). Atmos. Environ. 38, 4941–4956. https://doi.org/10.1016/j.atmosenv.2004.04.033.
Ochoa-Hueso, R., 2016. Nonlinear disruption of ecological interactions in response to nitrogen deposition. Ecology 97, 2802–2814. https://doi.org/10.1002/ecy.1521.
Ochoa-Hueso, R., Maestre, F.T., de los Ríos, A., Valea, S., Theobald, M.R., Vivanco, M.G., Manrique, E., Bowker, M.A., 2013. Nitrogen deposition alters nitrogen cycling and reduces soil carbon content in low-productivity semiarid Mediterranean ecosystems. Environ. Pollut. 179, 185–193. https://doi.org/10.1016/j.envpol.2013.03.060.
Padgett, P.E., Cook, H., Bytnerowicz, A., Heath, R.L., 2008. Foliar loading and metabolic assimilation of dry deposited nitric acid air pollutants by trees. J. Environ. Monit. 11, 75–84. https://doi.org/10.1039/B804338H.
Pan, Y.P., Wang, Y.S., Tang, G.Q., Wu, D., 2012. Wet and dry deposition of atmospheric nitrogen at ten sites in Northern China. Atmos. Chem. Phys. 12, 6515–6535. https://doi.org/10.5194/acp-12-6515-2012.
Pardo, L.H., Fenn, M.E., Goodale, C.L., Geiser, L.H., Driscoll, C.T., Allen, E.B., Baron, J.S., Bobbink, R., Bowman, W.D., Clark, C.M., Emmett, B., Gilliam, F.S., Greaver, T.L., Hall, S.J., Lilleskov, E.A., Liu, L., Lynch, J.A., Nadelhoffer, K.J., Perakis, S.S., Robin-Abbott, M.J., Stoddard, J.L., Weathers, K.C., Dennis, R.L., 2011. Effects of nitrogen deposition and empirical nitrogen critical loads for ecoregions of the United States. Ecol. Appl. 21, 3049–3082. https://doi.org/10.1890/10-2341.1.
Payne, R.J., Dise, N.B., Stevens, C.J., Gowing, D.J., Duprè, C., Dorland, E., Gaudnik, C., Bleeker, A., Diekmann, M., Alard, D., Bobbink, R., Fowler, D., Corcket, E., Mountford, J.O., Vandvik, V., Aarrestad, P.A., Muller, S., 2013. Impact of nitrogen deposition at the species level. Proc. Natl. Acad. Sci. 110, 984–987. https://doi.org/10.1073/pnas.1214299109.
Phoenix, G.K., Hicks, W.K., Cinderby, S., Kuylenstierna, J.C.I., Stock, W.D., Dentener, F.J., Giller, K.E., Austin, A.T., Lefroy, R.D.B., Gimeno, B.S., Ashmore, M.R., Ineson, P., 2006. Atmospheric nitrogen deposition in world biodiversity hotspots: the need for a greater global perspective in assessing N deposition impacts. Glob. Change Biol. 12, 470–476. https://doi.org/10.1111/j.1365-2486.2006.01104.x.

Poulter, B., Frank, D., Ciais, P., Myneni, R.B., Andela, N., Bi, J., Broquet, G., Canadell, J.G., Chevallier, F., Liu, Y.Y., Running, S.W., Sitch, S., van der Werf, G.R., 2014. Contribution of semi-arid ecosystems to interannual variability of the global carbon cycle. Nature 509, 600–603. https://doi.org/10.1038/nature13376.

Puchalski, M.A., Sather, M.E., Walker, J.T., Lehmann, C.M.B., Gay, D.A., Mathew, J., Robarge, W.P., 2011. Passive ammonia monitoring in the United States: comparing three different sampling devices. J. Environ. Monit. 13, 3156. https://doi.org/10.1039/c1em10553a.

Rao, L.E., Allen, E.B., 2010. Combined effects of precipitation and nitrogen deposition on native and invasive winter annual production in California deserts. Oecologia 162, 1035–1046. https://doi.org/10.1007/s00442-009-1516-5.

Rao, L.E., Allen, E.B., Meixner, T., 2010. Risk-based determination of critical nitrogen deposition loads for fire spread in southern California deserts. Ecol. Appl. 20, 1320–1335. https://doi.org/10.1890/09-0398.1.

Rao, L.E., Parker, D.R., Bytnerowicz, A., Allen, E.B., 2009. Nitrogen mineralization across an atmospheric nitrogen deposition gradient in Southern California deserts. J. Arid. Environ. 73, 920–930. https://doi.org/10.1016/j.jaridenv.2009.04.007.

R Core Team, 2017. R: A Language and Environment for Statistical Computing. R Foundation for Statistical Computing, Vienna, Austria. https://www.R-project.org.

Rao, P., Hutyra, L.R., Raciti, S.M., Finzi, A.C., 2013. Field and remotely sensed measures of soil and vegetation carbon and nitrogen across an urbanization gradient in the Boston metropolitan area. Urban Ecosyst. 16, 593–616. https://doi.org/10.1007/s11252-013-0291-6.

Redling, K., Elliott, E., Bain, D., Sherwell, J., 2013. Highway contributions to reactive nitrogen deposition: tracing the fate of vehicular NO_x using stable isotopes and plant biomonitors. Biogeochemistry 116, 261–274. https://doi.org/10.1007/s10533-013-9857-x.

Roadman, M.J., Scudlark, J.R., Meisinger, J.J., Ullman, W.J., 2003. Validation of Ogawa passive samplers for the determination of gaseous ammonia concentrations in agricultural settings. Atmos. Environ. 37, 2317–2325. https://doi.org/10.1016/S1352-2310(03)00163-8.

Salem, A.A., Soliman, A.A., El-Haty, I.A., 2009. Determination of nitrogen dioxide, sulfur dioxide, ozone, and ammonia in ambient air using the passive sampling method associated with ion chromatographic and potentiometric analyses. Air Qual. Atmos. Health 2, 133–145. https://doi.org/10.1007/s11869-009-0040-4.

Sather, M.E., Mathew, J., Nguyen, N., Lay, J., Golod, G., Vet, R., Cotie, J., Hertel, T., Aaboe, E., Callison, R., Adam, J., Keese, D., Freise, J., Hathcoat, A., Sakizzie, B., King, M., Lee, C., Oliva, S., San Miguel, G., Crow, L., Geasland, F., 2008. Baseline ambient gaseous ammonia concentrations in the Four Corners area and eastern Oklahoma, USA. J. Environ. Monit. 10, 1319. https://doi.org/10.1039/b807984f.

Sather, M.E., Slonecker, E.T., Mathew, J., Daughtrey, H., Williams, D.D., 2007. Evaluation of ogawa passive sampling devices as an alternative measurement method for the nitrogen dioxide annual standard in El Paso, Tex. Environ. Monit. Assess. 124, 211–221. https://doi.org/10.1007/s10661-006-9219-4.

Schade, J.D., Hobbie, S.E., 2005. Spatial and temporal variation in islands of fertility in the Sonoran Desert. Biogeochemistry 73, 541–553. https://doi.org/10.1007/s10533-004-1718-1.

Schumann, U., Huntrieser, H., 2007. The global lightning-induced nitrogen oxides source. Atmos. Chem. Phys. 7, 3823–3907. https://doi.org/10.5194/acp-7-3823-2007.

Schwede, D., Zhang, L., Vet, R., Lear, G., 2011. An intercomparison of the deposition models used in the CASTNET and CAPMoN networks. Atmos. Environ. 45, 1337–1346. https://doi.org/10.1016/j.atmosenv.2010.11.050.

Shen, W., Wu, J., Grimm, N.B., Hope, D., 2008. Effects of urbanization-induced environmental changes on ecosystem functioning in the Phoenix metropolitan region, USA. Ecosystems 11, 138–155. https://doi.org/10.1007/s10021-007-9085-0.

Simkin, S.M., Allen, E.B., Bowman, W.D., Clark, C.M., Belnap, J., Brooks, M.L., Cade, B.S., Collins, S.L., Geiser, L.H., Gilliam, F.S., Jovan, S.E., Pardo, L.H., Schulz, B.K., Stevens, C.J., Suding, K.N., Throop, H.L., Waller, D.M., 2016. Conditional vulnerability of plant diversity to atmospheric nitrogen deposition across the United States. Proc. Natl. Acad. Sci. 113, 4086–4091. https://doi.org/10.1073/pnas.1515241113.

Simkin, S.M., Lewis, D.N., Weathers, K.C., Lovett, G.M., Schwarz, K., 2004. Determination of sulfate, nitrate, and chloride in throughfall using ion-exchange resins. Water. Air. Soil Pollut. 153, 343–354. https://doi.org/10.1023/B:WATE.0000019958.59277.ed.

Sponseller, R.A., Hall, S.J., Huber, D.P., Grimm, N.B., Kaye, J.P., Clark, C.M., Collins, S.L., 2012. Variation in monsoon precipitation drives spatial and temporal patterns of Larrea tridentata growth in the Sonoran Desert. Funct. Ecol. 26, 750–758. https://doi.org/10.1111/j.1365-2435.2012.01979.x.

Sun, K., Tao, L., Miller, D.J., Pan, D., Golston, L.M., Zondlo, M.A., Griffin, R.J., Wallace, H.W., Leong, Y.J., Yang, M.M., Zhang, Y., Mauzerall, D.L., Zhu, T., 2017. Vehicle emissions as an important urban ammonia source in the United States and China. Environ. Sci. Technol. 51, 2472–2481. https://doi.org/10.1021/acs.est.6b02805.

Tulloss, E.M., Cadenasso, M.L., 2015. Nitrogen deposition across scales: hotspots and gradients in a California savanna landscape. Ecosphere 6, 1–12. https://doi.org/10.1890/ES14-00440.1.

United States Census Bureau, 2010. Census, Demographic Profile 1. https://www.census.gov/geo/maps-data/data/tiger.

United Nations, 2014. World Urbanization Prospects, the 2014 Revision.

Vitousek, P.M., Aber, J.D., Howarth, R.W., Likens, G.E., Matson, P.A., Schindler, D.W., Schlesinger, W.H., Tilman, D.G., 1997. Human alteration of the global nitrogen cycle: sources and consequences. Ecol. Appl. 7, 737–750. https://doi.org/10.1890/1051-0761(1997)007[0737:HAOTGN]2.0.CO;2.

Wang, G., Ostoja-Starzewski, M., 2004. Influence of topography on the Phoenix CO_2 dome: a computational study. Atmos. Sci. Lett. 5, 103–107. https://doi.org/10.1002/asl.67.

Weathers, K.C., Lovett, G.M., Likens, G.E., Caraco, N.F., 2000a. Cloudwater inputs of nitrogen to forest ecosystems in southern Chile: forms, fluxes, and sources. Ecosystems 3, 590–595.

Weathers, K.C., Lovett, G.M., Likens, G.E., Lathrop, R., 2000b. The effect of landscape features on deposition to Hunter Mountain, Catskill Mountains, New York. Ecol. Appl. 10, 528–540.

Weathers, K.C., Simkin, S.M., Lovett, G.M., Lindberg, S.E., 2006. Empirical modeling of atmospheric deposition in mountainous landscapes. Ecol. Appl. 16, 1590–1607.

Welter, J.R., Fisher, S.G., Grimm, N.B., 2005. Nitrogen transport and retention in an arid land watershed: influence of storm characteristics on terrestrial–aquatic linkages. Biogeochemistry 76, 421–440. https://doi.org/10.1007/s10533-005-6997-7.

Wesely, M.L., Hicks, B.B., 2000. A review of the current status of knowledge on dry deposition. Atmos. Environ. 34, 2261–2282. https://doi.org/10.1016/S1352-2310(99)00467-7.

Zbieranowski, A.L., Aherne, J., 2012. Ambient concentrations of atmospheric ammonia, nitrogen dioxide and nitric acid across a rural–urban–agricultural transect in southern Ontario, Canada. Atmos. Environ. 62, 481–491. https://doi.org/10.1016/j.atmosenv.2012.08.040.

Zhang, L., Wright, L.P., Asman, W. a. H., 2010. Bi-directional air-surface exchange of atmospheric ammonia: a review of measurements and a development of a big-leaf model for applications in regional-scale air-quality models. J. Geophys. Res. Atmos. 115. D20310. https://doi.org/10.1029/2009JD013589.

Zhu, J., He, N., Wang, Q., Yuan, G., Wen, D., Yu, G., Jia, Y., 2015a. The composition, spatial patterns, and influencing factors of atmospheric wet nitrogen deposition in Chinese terrestrial ecosystems. Sci. Total Environ. 511, 777–785. https://doi.org/10.1016/j.scitotenv.2014.12.038.

Zhu, L., Henze, D.K., Bash, J.O., Cady-Pereira, K.E., Shephard, M.W., Luo, M., Capps, S.L., 2015b. Sources and impacts of atmospheric NH_3: current understanding and frontiers for modeling, measurements, and remote sensing in North America. Curr. Pollut. Rep. 1, 95–116. https://doi.org/10.1007/s40726-015-0010-4.